The Plant Cell, Vol. 18, 747–763, March 2006, www.plantcell.org © 2006 American Society of Plant Biologists

The Chimeric *Arabidopsis* CYCLIC NUCLEOTIDE-GATED ION CHANNEL11/12 Activates Multiple Pathogen Resistance Responses [W] [OA]

Keiko Yoshioka,[a,b,1] Wolfgang Moeder,[a,b] Hong-Gu Kang,[a] Pradeep Kachroo,[a,2] Khaled Masmoudi,[c,d] Gerald Berkowitz,[c] and Daniel F. Klessig[a]

[a] Boyce Thompson Institute for Plant Research, Ithaca, New York 14853
[b] Department of Botany, University of Toronto, Toronto, Ontario M5S 3B2, Canada
[c] Department of Plant Science, University of Connecticut, Storrs, Connecticut 06269
[d] Center of Biotechnology of Sfax, Plant Molecular Genetics Unit, B.P.K. 3038, Sfax, Tunisia

To investigate the resistance signaling pathways activated by pathogen infection, we previously identified the *Arabidopsis thaliana* mutant *constitutive expresser of PR genes22* (*cpr22*), which displays constitutive activation of multiple defense responses. Here, we identify the *cpr22* mutation as a 3-kb deletion that fuses two cyclic nucleotide-gated ion channel (ATCNGC)–encoding genes, *ATCNGC11* and *ATCNGC12*, to generate a novel chimeric gene, *ATCNGC11/12*. Genetic, molecular, and complementation analyses suggest that ATCNGC11/12, as well as ATCNGC11 and ATCNGC12, form functional cAMP-activated ATCNGCs and that the phenotype conferred by *cpr22* is attributable to the expression of *ATCNGC11/12*. However, because overexpression of *ATCNGC12*, but not *ATCNGC11*, suppressed the phenotype conferred by *cpr22*, the development of this phenotype appears to be regulated by the ratio between ATCNGC11/12 and ATCNGC12. Analysis of knockout lines revealed that both ATCNGC11 and ATCNGC12 are positive mediators of resistance against an avirulent biotype of *Hyaloperonospora parasitica*. Through epistatic analyses, *cpr22*-mediated enhanced resistance to pathogens was found to require *NDR1*-dependent and *EDS1*/*PAD4*-dependent pathways. In striking contrast, none of these pathways was required for *cpr22*-induced salicylic acid accumulation or *PR-1* gene expression. These results demonstrate that *NDR1*, *EDS1*, and *PAD4* mediate other resistance signaling function(s) in addition to salicylic acid and pathogenesis-related protein accumulation. Moreover, the requirement for both *NDR1*-dependent and *EDS1*/*PAD4*-dependent pathways for *cpr22*-mediated resistance suggests that these pathways are cross-regulated.

INTRODUCTION

Plants contain a large number of defense systems that can be deployed to prevent pathogen infection. Whether these defense responses are successful appears to be determined largely by the intensity and rapidity of their activation. In certain plant–pathogen interactions, a strong and rapid defense response is triggered by the direct or indirect interaction between the products of a plant *R* gene and a pathogen avirulence (*avr*) gene (Flor, 1971; Keen, 1990). After this gene-for-gene–specific recognition, the inoculated leaves usually exhibit increased levels of salicylic acid (SA), the induction of several families of defense genes, including those encoding the pathogenesis-related (PR) proteins, and the development of a hypersensitive response (HR) (Hammond-Kosack and Jones, 1996). The HR is characterized by apoptotic-like cell death at the site(s) of pathogen entry and often the restriction of pathogen to the cells within and immediately surrounding the necrotic lesion(s). At later times after infection, increased SA levels and *PR* gene expression are detected in the uninoculated portions of the plant, concurrent with the development of systemic acquired resistance, a long-lasting, broad-based resistance to subsequent infection (Ryals et al., 1996; Dempsey et al., 1999).

Many studies have demonstrated that SA is a critical signaling molecule in the pathways leading to local and systemic resistance (Dempsey et al., 1999). To identify other components involved in the resistance pathway, various *Arabidopsis thaliana* mutants exhibiting altered responses to pathogen infection have been identified. One class displays constitutive *PR* gene expression, increased SA levels, and heightened resistance to virulent and avirulent pathogens; included in this group are the *lsd*, *cpr*, *ssi*, *acd*, *cim*, *hlm*, *cpn*, and *dnd* mutants (Yu et al., 1998; Glazebrook, 1999, 2001; Jambunathan et al., 2001; Balague et al., 2003). A subset of these mutants also spontaneously develop HR-like lesions. By contrast, a second class of mutants exhibit heightened disease susceptibility. Some of these, such as *npr1*/*nim1*, *sid1*/*eds5*, and *sid2*/*eds16*, fail to respond to exogenously supplied SA or to accumulate endogenous SA (Cao et al., 1994; Delaney et al., 1995; Shah et al., 1997; Nawrath and Metraux, 1999). In comparison, other enhanced susceptibility

[1] To whom correspondence should be addressed. E-mail yoshioka@botany.utoronto.ca; fax 416-978-5878.
[2] Current address: Department of Plant Pathology, University of Kentucky, Lexington, KY 40546.
The authors responsible for distribution of materials integral to the findings presented in this article in accordance with the policy described in the Instructions for Authors (www.plantcell.org) are: Keiko Yoshioka (yoshioka@botany.utoronto.ca) and Daniel F. Klessig (dfk8@cornell.edu).
[W] Online version contains Web-only data.
[OA] Open Access articles can be viewed online without a subscription.
Article, publication date, and citation information can be found at www.plantcell.org/cgi/doi/10.1105/tpc.105.038786.

mutants, including *pad4*, *eds1*, and *ndr1*, have lost *R* gene–mediated resistance to distinct groups of pathogens (Century et al., 1995; Glazebrook et al., 1996; Parker et al., 1996). Comparison of *R* gene structure with the requirement for *EDS1*, *PAD4*, or *NDR1* subsequently revealed that those R proteins with a coiled-coil, nucleotide binding site, and leucine-rich repeat (CC-NBS-LRR) structure generally require *NDR1* to signal defense responses, whereas those R proteins that have an N-terminal domain homologous with Toll and the interleukin-1 receptor followed by an NBS and LRR (TIR-NBS-LRR) usually require *EDS1* and *PAD4* (Aarts et al., 1998; Feys et al., 2001).

After *R* gene-mediated pathogen recognition, one of the most rapidly activated defense responses is a rapid, biphasic increase in reactive oxygen species, known as the oxidative burst. Another very early response is ion fluxes, including an influx of H^+ and Ca^{2+} and an efflux of K^+ and Cl^- (Atkinson et al., 1996). Of these ions, Ca^{2+} was shown to play a role in activating the oxidative burst after elicitor treatment (Chandra et al., 1997; Jabs et al., 1997; Sasabe et al., 2000) and in activating pathogen- or elicitor-induced cell death in tobacco (*Nicotiana tabacum*), cowpea (*Vigna unguiculata*), and soybean (*Glycine max*) (Atkinson et al., 1990; Levine et al., 1996; Xu and Heath, 1998; Sasabe et al., 2000). In addition, Ca^{2+} has been implicated in signaling SA-induced *PR* gene expression (Raz and Fluhr, 1992; Doke et al., 1996).

Consistent with a critical role for ion fluxes in defense signaling, three *Arabidopsis* mutants that constitutively express defense responses and spontaneously form HR-like lesions were found to contain defects in Ca^{2+}-related proteins. The *cpn1* (*bon1*) mutation disrupts a copine-encoding gene (Hua et al., 2001; Jambunathan et al., 2001). Copines are a newly identified class of Ca^{2+}-dependent phospholipid binding proteins that have been detected in diverse organisms ranging from ciliates to humans (Creutz et al., 1998). On the other hand, the *dnd1* and *hlm1*/*dnd2* mutations disrupt different members of the ATCNGC gene family (Clough et al., 2000; Balague et al., 2003; Jurkowski et al., 2004). ATCNGCs have been studied intensively in animals, in which they play important roles in the perception of light and smell (Zufall et al., 1994; Zagotta and Siegelbaum, 1996). These channels, which are thought to be heterotetrameric in structure (Zhong et al., 2003), facilitate the conductance of Ca^{2+}, K^+, Na^+, and other cations across the cell membrane (Kaupp and Seifert, 2002). ATCNGC subunits share many similarities with voltage-gated outward rectifying K^+-selective ion channel (Shaker) proteins, including a cytoplasmic N terminus, six membrane-spanning regions, a pore domain, and a cytoplasmic C terminus (Zagotta and Siegelbaum, 1996). However, ATCNGCs are gated primarily by the binding of cAMP or cGMP, rather than by voltage.

In *Arabidopsis*, the ATCNGC gene family consists of 20 members that have been divided into four groups based on sequence similarity (Maser et al., 2001). Cloning of *DND1* and *HLM1*/*DND2* revealed that they correspond to *ATCNGC2* and *ATCNGC4*, respectively (Clough et al., 2000; Balague et al., 2003, Jurkowski et al., 2004). These genes are highly related and belong to the same subgroup (Maser et al., 2001; Balague et al., 2003). Intriguingly, although mutations in these genes confer similar constitutive defense response phenotypes, some differences were noted. In particular, the *dnd1* mutation in *ATCNGC2* did not affect *R* gene–mediated resistance, whereas the *hlm1* mutation in *ATCNGC4* suppressed gene-for-gene resistance to certain pathogens but not others (Yu et al., 1998; Balague et al., 2003; Talke et al., 2003). Thus, the role played by ATCNGCs in defense signaling is currently unclear.

To identify the signaling components involved in activating defense responses after pathogen attack, we previously screened 4200 T-DNA–tagged lines from the Wassilewskija (Ws) ecotype for individuals that constitutively expressed *PR-1* (Yoshioka et al., 2001). One individual, designated *constitutive expresser of PR genes22* (*cpr22*), was identified. This mutant constitutively activated various defense responses, exhibited stunted growth with curly leaves, and displayed enhanced resistance to the virulent oomycete pathogen *Hyaloperonospora parasitica* (formerly *Peronospora parasitica*) Emco5. *cpr22* is a semidominant mutation that is lethal in the homozygous state unless the plant is grown under high RH. Here, we demonstrate that the phenotype conferred by *cpr22* is attributable to a deletion that generates a chimeric ATCNGC-encoding gene designated *ATCNGC11/12*. Genetic and molecular analyses suggest that the presence of *ATCNGC11/12* leads to the activation of SA-dependent, but *NDR1*- and *EDS1*/*PAD4*-independent, defense responses. By contrast, *cpr22*-mediated enhanced resistance appears to require both the *NDR1*- and *EDS1*/*PAD4*-mediated signaling pathways.

RESULTS

Isolation of the *cpr22* Mutation

The *cpr22* mutation was previously mapped to chromosome 2, ~2 centimorgan from *AthB102* (Yoshioka et al., 2001). However, because of a lack of polymorphisms between the Ws and Columbia (Col-0) ecotypes in this region, a second mapping population of 439 individuals was developed using the F2 progeny of a cross between *cpr22* and Landsberg *erecta*. Markers identified using the CEREON polymorphism database were used to localize *CPR22* to a 60-kb region spanned by BAC clones F11C10 and F13A10 (Figure 1A). Of the 16 open reading frames (ORFs) identified within this region, 9 were sequenced from *cpr22* and wild-type plants; comparison of these sequences identified a 3-kb deletion in a cluster of putative ATCNGC genes. The deletion generated a chimeric gene derived from *ATCNGC11* and *ATCNGC12* (Figure 1B).

Consistent with the structure of other ATCNGC-encoding genes, ATCNGC11 and ATCNGC12 are predicted to contain a cytoplasmic N terminus, six membrane-spanning segments, a pore domain, and a cytoplasmic C terminus that contains overlapping calmodulin binding and cyclic nucleotide binding domains (Kohler et al., 1999; Leng et al., 1999; Kohler and Neuhaus, 2000). This conserved structure also was observed in the chimeric *ATCNGC11/12* gene. Sequence comparison between *ATCNGC11/12*, *ATCNGC11*, and *ATCNGC12* suggested that a homologous recombination event occurred within the third membrane-spanning region, which fused the 5′ portion of *ATCNGC11* with the 3′ portion of *ATCNGC12*. Because a 222-bp stretch of this region is 100% homologous between *ATCNGC11* and *ATCNGC12*, the actual location of the recombination event cannot be determined.

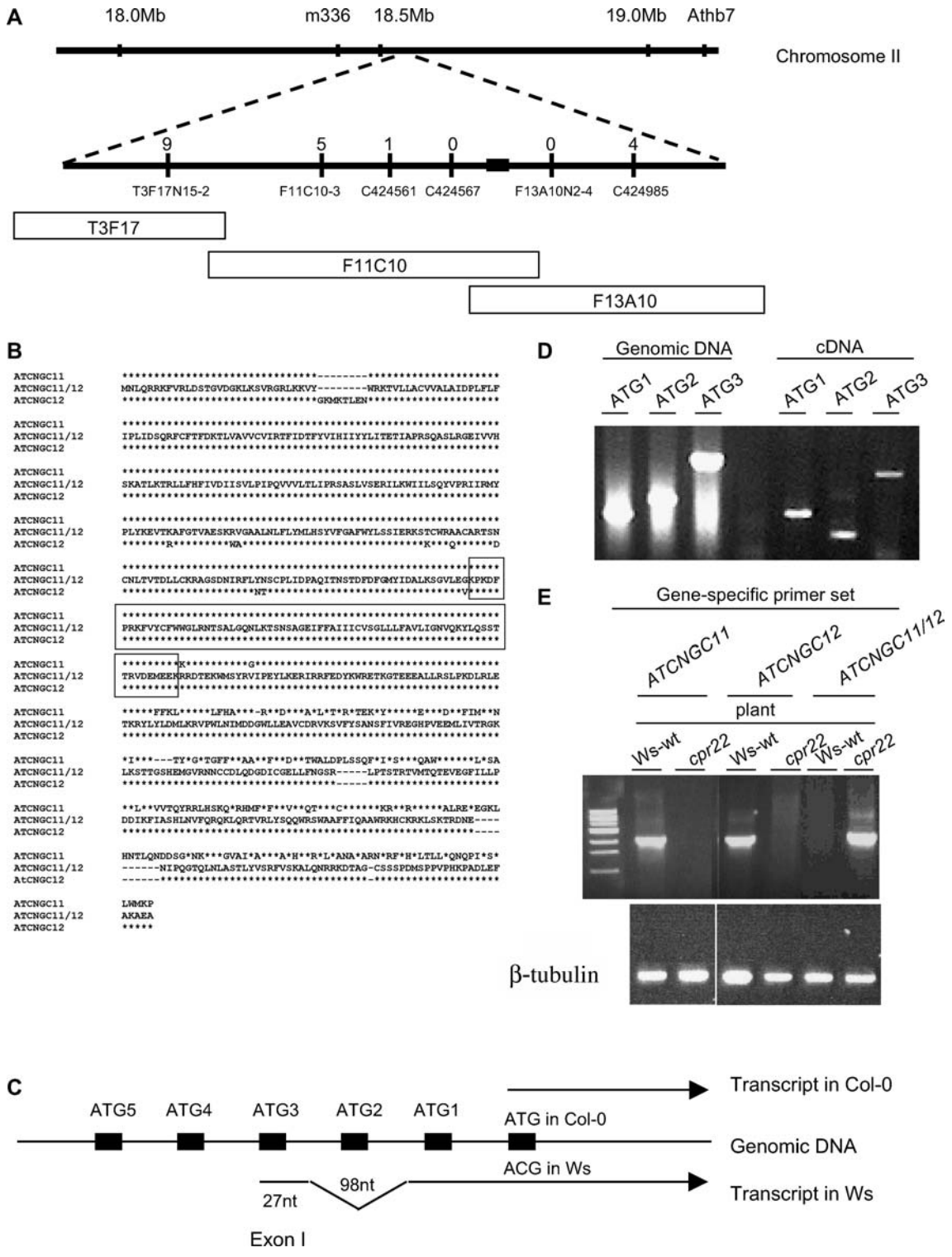

Figure 1. *cpr22* Is a 3-kb Deletion That Creates a Chimeric ATCNGC-Encoding Gene.

(A) Genetic and physical map of the *cpr22* locus on chromosome 2. The top line represents chromosome 2; the bottom line is a larger scale map of the *cpr22*-containing region, with various markers indicated below the line and the number of recombination events for each marker indicated above it. The location of the 3-kb deletion is indicated as a black box. BAC clones T3F17, F11C10, and F13A10, which span the *cpr22*-containing region, are represented as open boxes below the map.

The predicted ATG start codon for *ATCNGC11* in Col-0 corresponds to an ACG codon in the Ws allele. Thus, it was unclear whether *ATCNGC11*, and by extension the novel chimeric gene, was expressed in Ws plants. Alternatively, these proteins might be translated from an ATG farther 5′ in the predicted untranslated sequence. Analysis of the proposed 5′ region of the Ws *ATCNGC11* allele identified several ATG codons; however, without splicing of the RNA transcript, none would be in-frame with the downstream protein-encoding sequence. To assess whether ATCNGC11 was translated from one of these ATG codons, primers corresponding to sequences surrounding the first five upstream ATG codons were used for PCR analysis (Figure 1C). A fragment of the expected size was generated when a primer corresponding to the first ATG (ATG1; closest to the annotated translational start codon) was used with genomic DNA or cDNA as the template (Figure 1D). By contrast, primers corresponding to the second (ATG2) and third (ATG3) ATG codons only generated fragments of the expected size in the presence of genomic DNA; smaller than expected fragments were generated when cDNA was used as the template. Sequence analysis revealed that the fragment generated by the ATG2 primer was attributable to nonspecific amplification, whereas the fragment generated by the ATG3 primer lacked a 98-nucleotide region surrounding ATG2. This result, combined with the inability of primers corresponding to ATG codons upstream of ATG3 to generate product from the cDNA template (data not shown), suggested that *ATCNGC11* from Ws contains an extra exon and a 98-nucleotide intron upstream of the predicted start site for the Col-0 allele. The presence of a 27-nucleotide exon that is spliced in-frame with downstream sequences after removal of a 98-nucleotide intron was confirmed by sequencing ATG3-primed PCR products generated from genomic and cDNA templates (Figure 1C; data not shown). To determine whether the chimeric *ATCNGC11/12* gene also was expressed, cDNA prepared from *cpr22* plants was subjected to sequence analysis using the ATG3 primer. *ATCNGC11/12* was found to contain a full-length ORF, and based on semiquantitative RT-PCR analysis, it was expressed in *cpr22* to comparable levels as *ATCNGC11* and *ATCNGC12* in wild-type Ws plants (Figure 1E). Thus, we conclude that *ATCNGC11* and *ATCNGC11/12* are not pseudogenes.

ATCNGC11 and *ATCNGC12* Knockout Lines and Their F1 Progeny Display No Phenotypes Conferred by *cpr22* but Exhibit Reduced Resistance to an Avirulent Pathogen

Because *ATCNGC11* and *ATCNGC12* are expressed in wild-type plants but are combined into a chimeric gene in *cpr22*, the mutant phenotype could be attributable to the loss of one or both of these genes and/or to the expression of *ATCNGC11/12*. To begin addressing this question, *ATCNGC11* and *ATCNGC12* T-DNA insertion lines were obtained from the Salk Institute collection (T-DNA insertion lines Salk_026568 for *ATCNGC11* and Salk_092657 and Salk_092622 for *ATCNGC12*) and analyzed. Homozygous plants were obtained for all three knockout (KO) lines, and RT-PCR was used to confirm the absence of expression of the corresponding genes (see Supplemental Figure 1A online). All of the KO lines exhibited wild-type morphology and failed to spontaneously form lesions or constitutively express *PR-1* (Figures 2A and 2B). Their pathogen resistance status was analyzed using *H. parasitica* biotypes Noco2 and Emwa1. The Col-0 ecotype, which is the background for the Salk Institute T-DNA insertion lines, is susceptible to Noco2 and resistant to Emwa1. None of the three KO lines showed altered susceptibility to Noco2 compared with wild-type Col-0 plants (Table 1). However, resistance to Emwa1 was reduced in all three KO lines; 35 to 55% of the KO plants allowed sporangiophore development, with modest to high levels of sporangiophore development detected on ~20 to 30% of these plants (Figure 2C, Table 1). By contrast, no sporangiophores were observed on wild-type Col-0 plants. This reduction in resistance suggests that *ATCNGC11* and *ATCNGC12* are positive mediators of resistance against *H. parasitica* Emwa1.

Because *cpr22* plants lack full-length copies of both *ATCNGC11* and *ATCNGC12*, comparison of their phenotype with that of a double KO plant could be very informative. However, *ATCNGC11* and *ATCNGC12* are <1.5 kb apart, making the generation of a double KO via recombination extremely difficult. Using RNA interference to create a line specifically silenced for *ATCNGC11* and *ATCNGC12* also would be problematic, because there are 20 members in the *ATCNGC* family and some of

Figure 1. (continued).

(B) Amino acid sequence alignment of ATCNGC11, ATCNGC11/12, and ATCNGC12 from the Ws ecotype. The deduced amino acid sequence for ATCNGC11/12 is in the middle; amino acid residues in ATCNGC11 and/or ATCNGC12 that are identical to those of ATCNGC11/12 are represented as asterisks, whereas residues that differ are indicated above or below the line. The boxed region contains sequences that are identical in all three proteins. Because the predicted ATCNGC11/12 sequence is identical to ATCNGC11 upstream of the boxed sequence and to ATCNGC12 downstream of this sequence, the homologous recombination event that created ATCNGC11/12 likely occurred within this region.

(C) Scheme of the 5′ translated and untranslated regions of the Col-0 and Ws alleles of *ATCNGC11.* To investigate the position of the translational start codon in the Ws allele of *ATCNGC11*, RT-PCR analysis was performed with primers corresponding to five ATG codons near the predicted translational start codon of the Col-0 allele. ATG1 to ATG5 are depicted as black boxes on the genomic DNA. This analysis suggested that the transcript for the Ws allele (bottom arrow) contains an extra 98-nucleotide intron and 27-nucleotide exon that are not present in the transcript of the Col-0 allele (top arrow).

(D) PCR analysis of *ATCNGC11* (Ws ecotype). Forward primers ATG1, ATG2, and ATG3, which correspond to the first three ATG codons within the predicted 5′ untranslated region of *ATCNGC11*, were tested for their ability to generate a product using genomic DNA or cDNA from wild-type Ws plants as the template in combination with the ATCNGC11-specific reverse primer UD1R1. ATG1 is closest to the annotated translational start codon, and ATG3 is farther upstream. The products were resolved on an agarose gel and stained with ethidium bromide. See text for additional information.

(E) Semiquantitative RT-PCR analysis of *ATCNGC11*, *ATCNGC12*, and *ATCNGC11/12* transcript levels in wild-type Ws and *cpr22* homozygous plants using gene-specific primers. The products were resolved on an agarose gel and stained with ethidium bromide. β-Tubulin was used as a loading control.

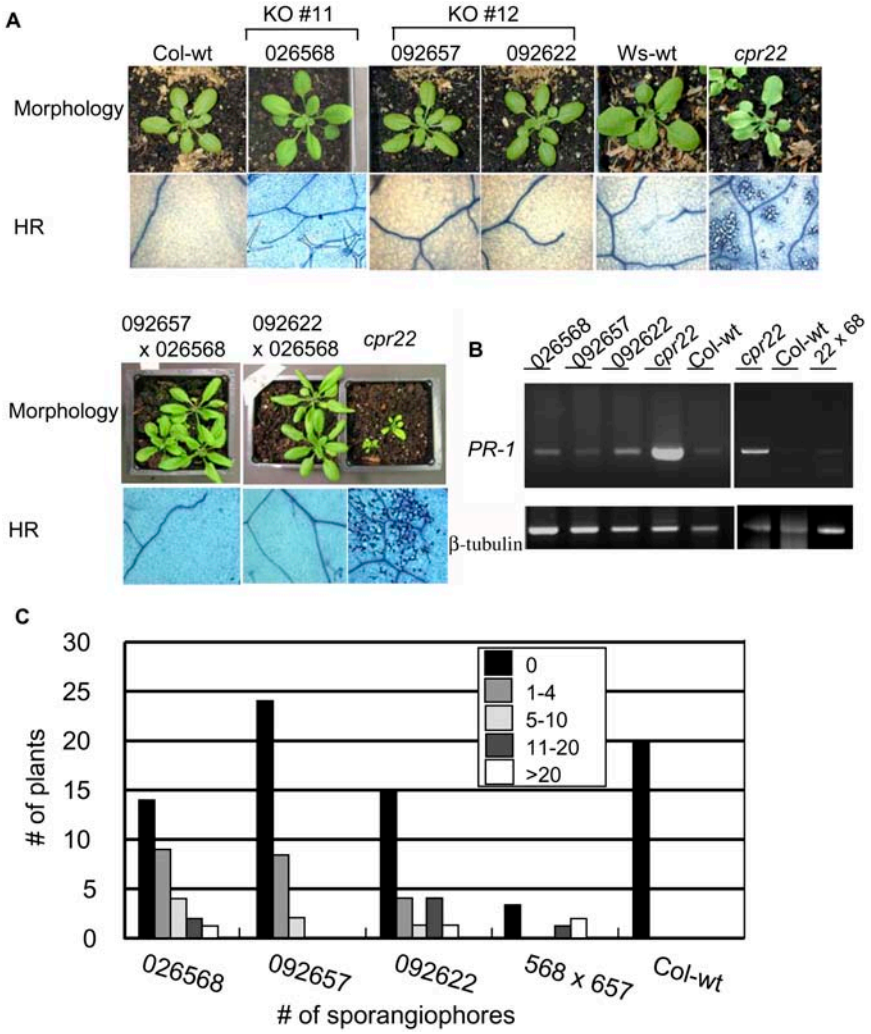

Figure 2. KO Lines of *ATCNGC11* (Salk_026568), *ATCNGC12* (Salk_ 092657 and Salk_092622), and Their F1 Progeny Display No Phenotypes Conferred by *cpr22* but Exhibit Reduced Resistance to *H. parasitica* Emwa1.

(A) Morphological phenotype and spontaneous cell death in wild-type Col-0 and Ws plants, the *cpr22* mutant, *ATCNGC11* and *ATCNGC12* KO lines, and their F1 progeny. Plants were photographed 3 weeks after planting for single KO lines and 4 weeks after planting for F1 progeny. Lesion formation was monitored microscopically in leaves of 25-d-old plants after trypan blue staining.

(B) RT-PCR analysis for *PR-1* gene expression. PR1-F and PR1-R primers were used for the detection of *PR-1* gene expression, and β-tubulin-5′ and β-tubulin-3′ primers were used for the detection of β-tubulin gene expression.

(C) Infection with *H. parasitica* Emwa1. Seven-day-old seedlings were inoculated with *H. parasitica* Emwa1 (10^6 spores/mL). At 6 d after inoculation, two cotyledons per plant were analyzed with a microscope and categorized into one of five categories (0, 1 to 4, 5 to 10, 11 to 20, or >20) depending on the number of sporangiophores observed on the two cotyledons. Experiments were performed four times with similar results.

these genes are highly similar in their DNA sequences (Maser et al., 2001). Given the difficulty involved in obtaining a double KO, we decided to cross the *ATCNGC11* and *ATCNGC12* KO lines and monitor the phenotype of the F1 progeny. The *cpr22* mutation is semidominant and leads to a readily visible phenotype in the heterozygous state (one copy each of *ATCNGC11*, *ATCNGC12*, and *ATCNGC11/12*) when grown under normal RH conditions. Thus, if the phenotype conferred by *cpr22* is attributable to the loss of one copy of *ATCNGC11* and *ATCNGC12*, rather than to the expression of *ATCNGC11/12*, the F1 progeny of crosses between the KO lines should exhibit a phenotype like that conferred by *cpr22*. F1 plants from crosses between Salk_026568 (ATCNGC11) and Salk_092657 (ATCNGC12) or between Salk_026568 (ATCNGC11) and Salk_092622 (ATCNGC12) were created by reciprocal cross-pollination. To confirm heterozygosity, the T-DNA insertion in each gene was analyzed by PCR using gene-specific primers as well as a primer specific for the T-DNA sequence (see Supplemental Figure 1B online). All of the F1 plants exhibited wild-type morphology and, like the single KO lines, failed to spontaneously form lesions or

Table 1. Resistance Status of Single and Double Knockout Plants to *H. parasitica*

Isolate	Plant Line[a]	Total No. of Plants	No. of Infected Plants[b]	Infected Plants (%)
Noco2 (Vir)	026568	28	24	85.7
	092657	17	13	76.5
	092622	20	17	85.0
	568 × 57	7	6	85.7
	Col wild type	14	12	85.7
Emwal (Avr)	026568	30	16	53.3
	092657	34	10	29.4
	092622	27	10	37.0
	568 × 57	6	3	50.0
	Col wild type	20	0	0.0

[a] 568 × 57; F1 of cross-pollination between Salk_026568 and Salk_092657.
[b] Based on formation of sporangiophores.

constitutively express *PR-1* (Figures 2A and 2B). Therefore, the phenotype conferred by *cpr22* is not attributable simply to the loss of one copy each of these two ATCNGC genes. Analysis of a small number of plants (because of the limited number of F1 seeds) revealed comparable levels of susceptibility to *H. parasitica* Noco2 and exhibited similarly reduced resistance to Emwa1 as the single KO lines (Table 1, Figure 2C). Because the F1 plants contain a single copy of *ATCNGC11* and *ATCNGC12*, and the parent KO lines contain two copies of either *ATCNGC11* or *ATCNGC12*, these results suggest that these ATCNGCs are at least partially redundant for resistance.

Expression of *ATCNGC11/12* Is Required for the Phenotype Conferred by *cpr22*

The results with the F1 plants suggest that the phenotype conferred by *cpr22*, at least in *cpr22/CPR22* heterozygous plants, is not attributable to the loss of one functional copy of *ATCNGC11* or *ATCNGC12*. Whether expression of *ATCNGC11/12* leads to the phenotype conferred by *cpr22* was then tested by transforming diploid wild-type Ws plants with *ATCNGC11/12* driven by the powerful cauliflower mosaic virus (CaMV) 35S promoter. By 4 weeks after planting, these transgenic plants developed a phenotype similar to that of *cpr22* heterozygous plants, including stunted growth, curly leaves, spontaneous lesion formation and constitutive *PR-1* expression, whereas transgenic plants expressing *35S-ATCNGC11* or *35S-ATCNGC12* constructs were indistinguishable from untransformed control plants (Figure 3A; see Supplemental Figure 2 online). Further arguing that expression of *ATCNGC11/12* leads to the phenotype conferred by *cpr22*, transient expression of CaMV 35S-driven *ATCNGC11/12*, but not *ATCNGC11* or *ATCNGC12*, induced HR-like cell death in *Nicotiana benthamiana* (Figure 3B). Analysis of *cpr22/CPR22/CPR22* triploid plants (created by crossing a *cpr22* homozygous mutant with a tetraploid CS3432 plant [Col-0 ecotype]), however, revealed that expression of *ATCNGC11/12* does not necessarily lead to the phenotype conferred by *cpr22*. All 12 F1 progeny from independent crosses displayed wild-type morphology and did not constitutively express *PR-1* (Figure 3C). Seed development in the triploid plants, however, was arrested in ambient RH growth conditions and was restored to nearly normal levels by high RH growth conditions. One possible explanation for the different phenotypes of *35S-ATCNGC11/12* transgenic plants and the triploid plants is that the phenotype conferred by *cpr22* is determined by the ratio between the expression of *ATCNGC11/12* and the wild-type copy(s) of *ATCNGC11* and/or *ATCNGC12*. Because *ATCNGC11/12* expression is driven by its endogenous (*ATCNGC11*) promoter in the triploid plants, its expression level may not be sufficient to result in the phenotype conferred by *cpr22* in the presence of two copies of wild-type *ATCNGC11* and *ATCNGC12*. By contrast, stronger expression of *ATCNGC11/12* from the 35S promoter in transgenic plants might overcome the presence of the wild-type genes.

ATCNGC12 Suppresses the Phenotype Conferred by *cpr22* in a Dosage-Dependent Manner

To investigate whether the phenotype conferred by *cpr22* is regulated by the ratio between ATCNGC11/12 and ATCNGC11 and/or ATCNGC12, we tested whether the phenotype conferred by *cpr22* was affected by increasing the dosage of the wild-type genes. More than 30 independent T1 lines were generated from *cpr22* heterozygous plants transformed with an ~3.3-kb genomic copy of *ATCNGC12*. Strikingly, the phenotype of many of these plants was nearly identical to that of wild-type plants. Although these T1 plants were slightly stunted, they did not develop spontaneous lesions or constitutively express *PR-1* under normal RH growth conditions (Figure 4A). Three independent T1 lines also were generated from *cpr22* homozygous plants transformed with the genomic copy of *ATCNGC12*. Plants from all of these lines grew in low RH conditions without lethality, and the severity of stunting, leaf curling, and spontaneous lesion formation was similar to that of *cpr22* heterozygous plants (Figure 4A). Analysis of T2 progeny from all of the T1 lines transformed with *ATCNGC12* confirmed that expression of this transgene suppressed *cpr22*-induced stunting, spontaneous lesion formation, and constitutive *PR-1* expression in a dose-dependent manner. Of 25 T2 plants from a self-pollinated *cpr22* homozygous line expressing *ATCNGC12*, 4 progeny were slightly stunted but otherwise wild type in morphology, 15 developed a phenotype similar to that of *cpr22* heterozygous plants, and 6 died (consistent with the *cpr22* homozygous phenotype); these results conform with the predicted 1:2:1 ratio ($\chi^2 = 1.32$; $0.80 > P > 0.50$) for a single, semidominant locus. Analysis of 70 T2 progeny from a self-pollinated *cpr22* heterozygous line expressing *ATCNGC12* identified 43 progeny with the nearly wild-type morphology, 22 with a phenotype similar to that of *cpr22* heterozygous plants, and 5 that died. These results are consistent with an 11:4:1 ratio ($\chi^2 = 1.78$; $0.5 > P > 0.20$), which would be predicted if the transgene segregates independently of the *CPR22* locus and two doses of *ATCNGC12* are sufficient to confer the wild-type or nearly wild-type morphology.

By contrast, transformation of *cpr22* heterozygous plants with an ~5.5-kb genomic copy of *ATCNGC11* produced only two independent T1 lines, despite multiple attempts. The T1 lines and their subsequent T2 progeny showed *cpr22*-like curly leaves, spontaneous HR development, and *PR-1* gene expression

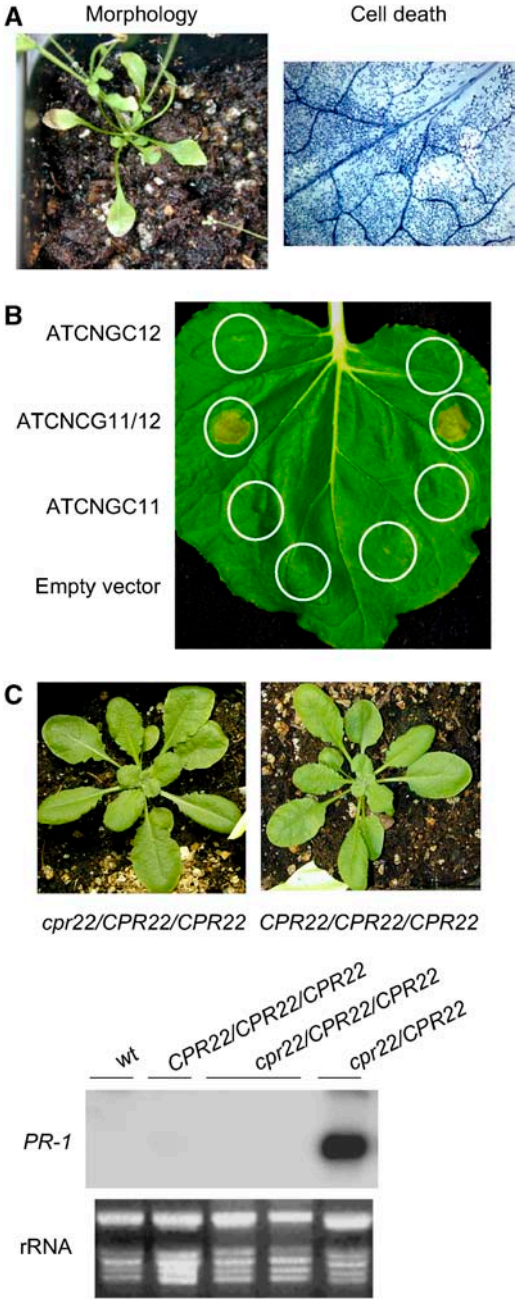

Figure 3. Expression of *ATCNGC11/12* Is Required for the Phenotype Conferred by *cpr22*.

(A) Mutant morphology and spontaneous lesion formation in wild-type Ws plants transformed with *ATCNGC11/12* driven by the CaMV 35S promoter. Plants were grown on soil and photographed at 4 weeks after planting . Microscopic analysis of trypan blue–stained leaves from these plants revealed intensely stained areas of dead cells.

(B) Transient expression of *ATCNGC12*, *ATCNGC11/12*, or *ATCNGC11* in *N. benthamiana*. Agrobacteria containing an empty vector (pMBP3) or a vector containing *ATCNGC12*, *ATCNGC11*, or *ATCNGC11/12* driven by the CaMV 35S promoter were infiltrated into *N. benthamiana* leaves. The infiltrated areas are circled. Leaves were photographed at 3 d after infiltration and showed lesion formation only with *ATCNGC11/12* expression.

(C) Phenotypes of wild-type triploid (*CPR22/CPR22/CPR22*) and a triploid *cpr22/CPR22/CPR22* plant. The plants were grown on soil and photographed at 3 weeks after planting (top). RNA gel blot analysis was performed using 8 μg of total RNA harvested from 3-week-old plants (bottom). Ethidium bromide staining of rRNA served as a loading control.

(Figure 4A; data not shown). Although these results suggested that *ATCNGC11* cannot complement the phenotype conferred by *cpr22*, it should be noted that the level of *ATCNGC11* transgene expression, and that of the *ATCNGC12* transgene, cannot be monitored because they are indistinguishable from those of the corresponding endogenous genes.

To determine whether increased expression of *ATCNGC12* suppresses other aspects of the phenotype conferred by *cpr22*, we monitored the ability of this transgene to compromise *cpr22*-mediated disease resistance in *Arabidopsis* and HR development in *N. benthamiana*. Analysis of T2 progeny from a *cpr22* heterozygous plant transformed with *ATCNGC12* revealed that resistance to *H. parasitica* Emco5 was suppressed (data not shown). Coexpression analysis using green fluorescent protein–tagged ATCNGC11/12, ATCNGC11, and ATCNGC12 in *N. benthamiana* indicated that ATCNGC12 also reduced lesion formation caused by ATCNGC11/12, but only when both were expressed and/or present at similar levels (Figure 4C). By contrast, neither the empty vector nor ATCNGC11 affected lesion formation when present at a similar (or lesser) level as ATCNGC11/12.

Functional Analysis of ATCNGC11, ATCNGC12, and ATCNGC11/12

Native ATCNGCs in animals are heterotetrameric proteins composed of more than one ATCNGC gene product (Zhong et al., 2003). Some studies have suggested that native plant ATCNGC channel complexes also are composed of multiple subunits expressed from different ATCNGC genes. In addition, Arazi et al. (1999) found that overexpression of a plant ATCNGC could enhance the uptake of one cation and reduce the uptake of another in transgenic plants. Together, these results are consistent with a model positing that native plant ATCNGC channels are heteromeric and that altered expression of a specific ATCNGC subunit could alter the assembly of the native channel complex and change its conductance profile. Thus, provided that ATCNGC11/12 is capable of forming channels, the phenotype conferred by *cpr22* might be caused by altered cation concentrations attributable to the presence of heteromeric channels containing ATCNGC11/12 and ATCNGC12 or other ATCNGC family members.

To determine whether *ATCNGC12*, *ATCNGC11*, and *ATCNGC11/12* encode functional cation channels, heterologous expression assays were performed in the *trk1,2* yeast mutant. This mutant lacks the functional K^+ uptake proteins TRK1 and TRK2 (Gaber et al., 1988; Ko and Gaber, 1991). Reduced cation uptake in this mutant results in a hyperpolarized (inside negative) membrane potential and concomitant hypersensitivity to the cationic antibiotic hygromycin B. However, the *trk1,2* yeast

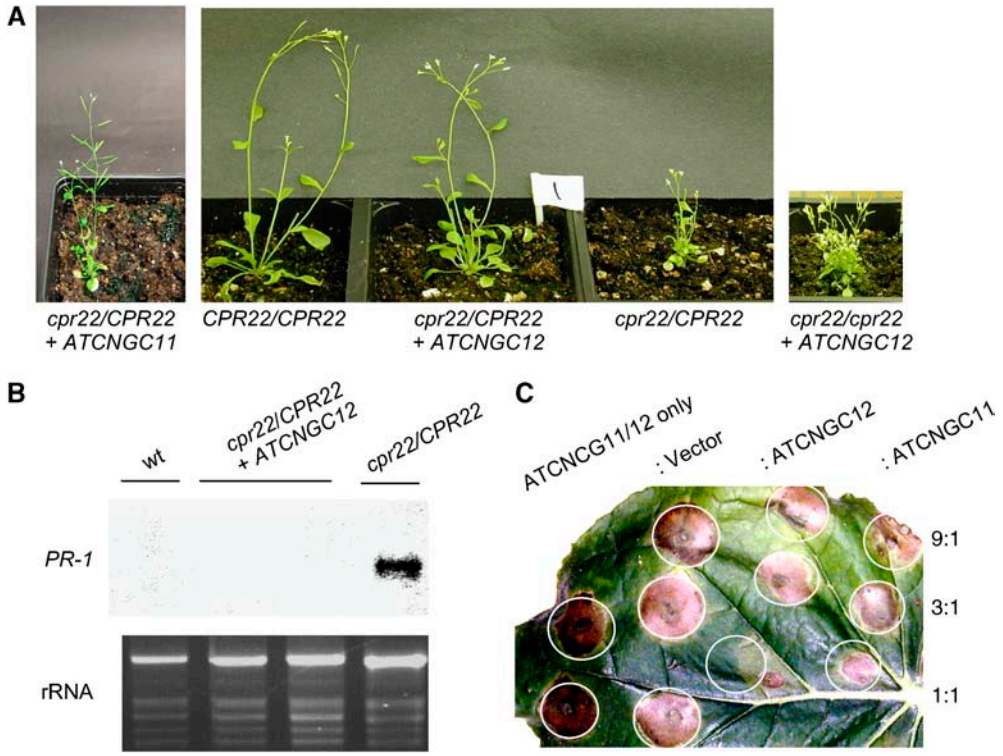

Figure 4. The Severity of the Phenotype Conferred by *cpr22* Is Determined by the Ratio between *ATCNGC11/12* and *ATCNGC12*.

(A) Morphological phenotypes of wild-type (*CPR22/CPR22*) and *cpr22* (*cpr22/CPR22*) plants, as well as those of a *cpr22* heterozygous plant transformed with an ~5.5-kb genomic copy of *ATCNGC11* (*cpr22/CPR22* + *ATCNGC11*) and *cpr22* heterozygous and homozygous plants transformed with an ~3.3-kb genomic copy of *ATCNGC12* (*cpr22/CPR22* + *ATCNGC12* and *cpr22/cpr22* + *ATCNGC12*, respectively). The plants were grown on soil and photographed at 4 weeks after planting.

(B) *PR-1* gene expression in wild-type (*CPR22/CPR22*) plants, the *cpr22/CPR22* mutant, and a *cpr22/CPR22* mutant transformed with *ATCNGC12*. RNA gel blot analysis was performed using 8 μg of total RNA harvested from 3-week-old plants. Ethidium bromide staining of rRNA served as a loading control.

(C) Transient coexpression analysis of *ATCNGC11*, *ATCNGC12*, or *ATCNGC11/12* in *N. benthamiana*. Agrobacteria containing a *35S-ATCNGC11/12* construct in the pMBP3 vector were infiltrated alone or coinfiltrated with differing concentrations of agrobacteria containing either an empty vector or a *35S-ATCNGC12* or *35S-ATCNGC11* construct into *N. benthamiana* leaves. The ratios of *ATCNGC11/12* to empty vector, *ATCNGC12*, and *ATCNGC11* are designated at right. The infiltrated leaf was photographed at 3 d after infiltration. The expression level of each gene was confirmed and monitored by protein gel blot analysis using a specific antibody against green fluorescent protein and by fluorescent microscopic observation.

mutant can grow in medium containing hygromycin B plus K^+ if a cation transport protein capable of conducting K^+ is expressed in the mutant (Madrid et al., 1998; Bihler et al., 2002). Moreover, Mercier et al. (2004) recently showed that expression of plant ATCNGCs complemented the hypersensitivity of *trk1,2* growth (around a filter disk containing K^+) to hygromycin B.

We used the functional assay developed by Mercier et al. (2004) to test the cyclic nucleotide-dependent inward cation conductance (i.e., ATCNGC function) of ATCNGC11, ATCNGC12, and ATCNGC11/12. The *trk1,2* mutant transformed with the empty plasmid (control) did not grow around a K^+-containing filter disk on medium containing hygromycin B either in the absence or presence of cAMP (Figure 5). By contrast, ATCNGC11, ATCNGC12, and the chimeric ATCNGC11/12 complemented the growth of *trk1,2*. However, the growth of the mutant yeast expressing ATCNGC11/12 was less vigorous than that of mutants expressing either *ATCNGC11* or *ATCNGC12*.

One of the defining attributes of members of the ATCNGC family is the (direct) activation of currents by the ligand cAMP (Kaupp and Seifert, 2002). As shown most clearly by mutant yeast expressing *ATCNGC11* and *ATCNGC12*, addition of a lipophilic analog of cAMP to the growth medium increased colony growth around the filter disk (Figure 5), thus demonstrating that these proteins are ATCNGCs. Although cAMP clearly stimulated the growth of mutant yeast expressing chimeric *ATCNGC11/12*, again, growth was less vigorous than in yeast expressing the wild-type *ATCNGC*s. Addition of dibutyryl-cGMP did not enhance the growth of yeast expressing *ATCNGC11*, *ATCNGC12*, or *ATCNGC11/12* (data not shown); thus, it appears that these channels are activated solely by cAMP and not by cGMP. Interestingly, Lemtiri-Chlieh and Berkowitz (2004) recently documented the presence of native ATCNGCs in mesophyll and guard cells of *Arabidopsis* plants activated by cAMP but not by cGMP.

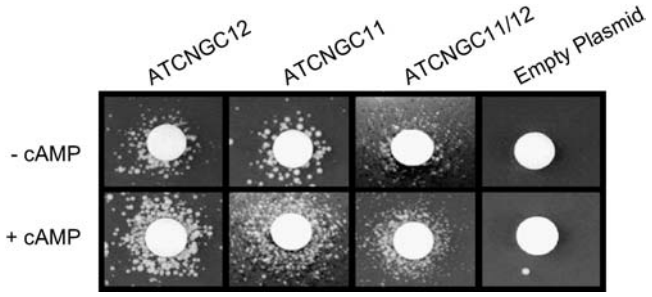

Figure 5. *ATCNGC11*, *ATCNGC12*, and *ATCNGC11/12* Encode Functional Cyclic Nucleotide-Gated Cation Channels.

Complementation of hygromycin hypersensitivity of *trk1,2* yeast by transfection with empty plasmid, *ATCNGC11*, *ATCNGC12*, or *ATCNGC11/12*. After transformation, the ability of yeast cells to grow around a filter disk containing 3 M KCl (center of each panel) on solid YPGal medium containing 0.07 mg/mL hygromycin B in the presence or absence of 100 μM cAMP was monitored. Photographs were taken after 3 d of growth. Data shown are representative results obtained with this assay in four independent experiments.

Lesion Formation Is Not Impaired in *cpr22* Plants Inoculated with an Avirulent Pathogen

Previously, three *Arabidopsis* ATCNGC mutants were isolated, *dnd1* and *hlm1*/*dnd2* (Clough et al., 2000; Balague et al., 2003; Jurkowski et al., 2004). Although there are several differences in their phenotypes, all three mutants display delayed and/or suppressed HR cell death upon infection with various avirulent pathogens (Yu et al., 1998; Balague et al., 2003). Therefore, we tested whether HR cell death is altered in *cpr22* plants. After inoculation with the avirulent pathogen *Pseudomonas syringae* pv *tomato* DC3000 expressing *avrRpt2*, both visual inspection and microscopic analysis with trypan blue revealed that the kinetics of HR cell death were comparable in wild-type Ws and *cpr22* plants. As reported previously (Yoshioka et al., 2001), *cpr22* is humidity-sensitive. High RH (>95%) suppresses the phenotype conferred by *cpr22*/*CPR22* almost completely, and relatively high RH (70%) causes a milder phenotype, including less stunting and lesion formation. To facilitate the observation of pathogen-induced HR in *cpr22* plants, all plants were grown under 70% RH. Therefore, spontaneous lesion formation in *cpr22* at 0 d after inoculation was milder than that under normal RH conditions (RH of 55%; compare Figure 6, 0 d after inoculation, with Figure 7B). Cell death was first detected ~24 h after inoculation and became more pronounced by 2 d after inoculation in both wild-type and *cpr22* plants (Figure 6; data not shown). Thus, *cpr22*, unlike *dnd1* and *hlm1*/*dnd2*, is capable of developing a normal HR in response to infection with an avirulent pathogen.

Many *cpr22*-Associated Phenotypes Are Independent of *EDS1*, *PAD4*, and *NDR1*

To determine whether *cpr22* constitutively activates *PR-1* expression, spontaneous lesion formation, SA accumulation, and enhanced resistance to *H. parasitica* Emco5 via defense signaling pathways used during *R* gene–mediated resistance, we previously crossed *cpr22* plants with the *ndr1-1* mutant (Yoshioka et al., 2001). Analysis of the resultant progeny indicated that *NDR1* is required for *cpr22*-mediated resistance to *H. parasitica*. To expand this analysis and also to determine whether any of the other *cpr22*-associated phenotypes are dependent on *PAD4* or *EDS1*, we crossed a *cpr22*/*CPR22* plant with homozygous *pad4-1* and *ndr1-1* plants. In addition, a *cpr22* homozygous plant grown under high RH was crossed with a homozygous *eds1-1* mutant. In the F1 generation, ~50% of the progeny from the *pad4-1* and *ndr1-1* crosses exhibited stunted growth, curly leaves, and constitutive *PR-1* expression, consistent with the semidominant nature of the *cpr22* mutation (Table 2). By contrast, the remaining ~50% of the plants were morphologically wild type. All F1 progeny from the cross between *cpr22* homozygous plants and the *eds1-1* mutant were stunted and constitutively expressed *PR-1*, as expected.

After allowing the stunted F1 progeny from each cross to self-pollinate, the F2 progeny were analyzed. For each cross, ~25% of the F2 progeny died at ambient (low) RH, ~50% exhibited the phenotype conferred by *cpr22*, as indicated by stunted growth, curly leaves, and constitutive *PR-1* expression, and ~25% were morphologically wild type (Table 2). This 1:2:1 ratio suggests that development of these *cpr22*-associated phenotypes is independent of *NDR1*, *PAD4*, and *EDS1*. These results were confirmed using F3 progeny analysis and cleaved-amplified polymorphic sequence (CAPS) markers to identify F2 plants heterozygous for *cpr22* and homozygous for *ndr1-1*, *pad4-1*, or *eds1-1*. As expected, the *cpr22 ndr1-1*, *cpr22 eds1-1*, and *cpr22 pad4-1* double mutants were all stunted, although the phenotype of *cpr22 pad4-1* plants was somewhat less severe (Figure 7A). Trypan blue staining revealed that these double mutants developed similar numbers of spontaneous HR-like lesions as *cpr22* single mutants (Figure 7B). They also constitutively expressed *PR-1* to comparable levels as *cpr22* single mutant plants (Figure 7C). Together, these results demonstrate that *PAD4*, *EDS1*, and *NDR1* are not required for *cpr22*-associated lethality, stunting, spontaneous lesion formation, or constitutive *PR-1* expression.

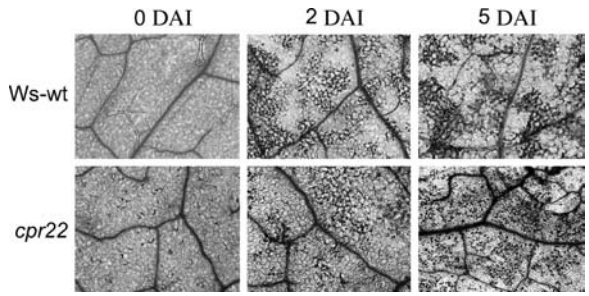

Figure 6. The *cpr22* Mutant Develops a Normal HR after Infection with an Avirulent Pathogen.

Microscopic analysis of trypan blue–stained leaves from ~20-d-old wild-type Ws and *cpr22*/CPR22 plants. After inoculation with *P. syringae* pv *tomato* carrying *avrRpt2*, leaves were photographed at 0, 2, or 5 d after inoculation (DAI).

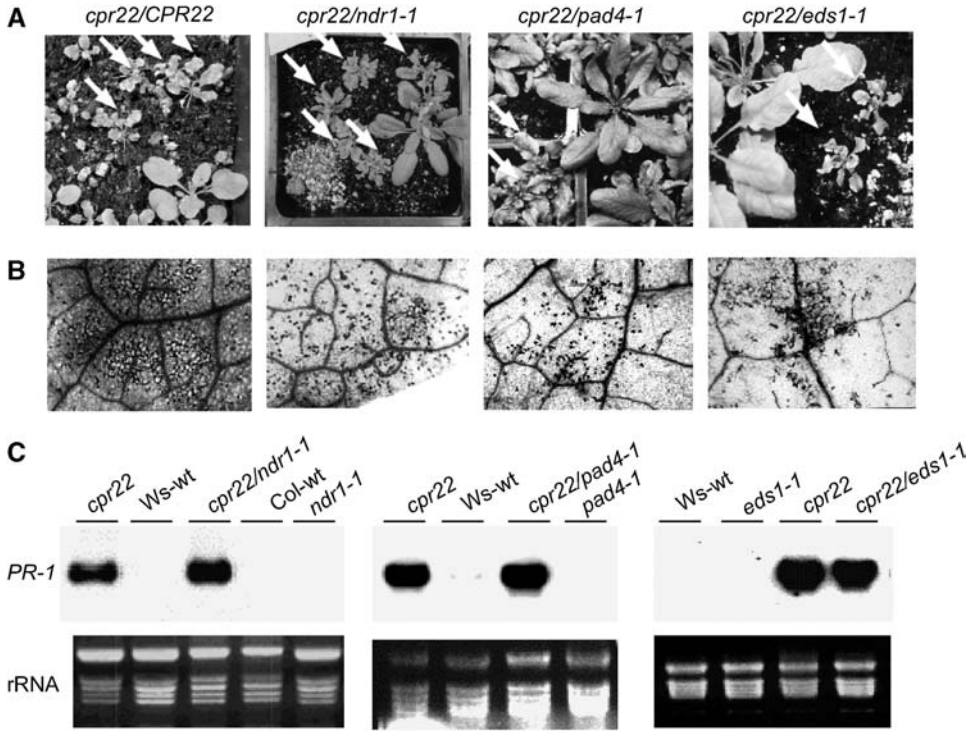

Figure 7. *PAD4*, *EDS1*, and *NDR1* Are Not Required for *cpr22*-Mediated Stunting, Spontaneous Lesion Formation, or *PR-1* Gene Expression.

(A) Comparison of the morphology displayed by segregating F3 progeny from a self-pollinated *cpr22/CPR22* mutant plant and those of self-pollinated *cpr22/CPR22* plants homozygous for *ndr1-1*, *pad4-1*, or *eds1-1* (*cpr22 ndr1-1*, *cpr22 pad4-1*, and *cpr22 eds1-1*, respectively). Arrows indicate plants containing the *cpr22/CPR22* genotype (based on molecular and progeny analyses); regardless of the allele at the *NDR1*, *PAD4*, or *EDS1* locus, these plants displayed stunted growth and curly leaves. Plants were photographed at 4 weeks after planting.

(B) Microscopic analysis of trypan blue–stained leaves from 3-week-old F3 progeny heterozygous for *cpr22* as well as from *cpr22/CPR22* plants homozygous for *ndr1-1*, *pad4-1*, or *eds1-1*. Darkly stained areas indicative of cell death were detected in all sets of progeny.

(C) Expression of the *PR-1* gene in *CPR22/CPR22* (Ws-wt and Col-wt) plants, heterozygous *cpr22/CPR22* (*cpr22*) and homozygous *ndr1-1*, *pad4-1*, or *eds1-1* single mutant plants, and *cpr22* heterozygous and *ndr1-1*, *pad4-1*, or *eds1-1* homozygous double mutants. RNA gel blot analysis was performed using 8 μg of total RNA harvested from 3-week-old soil-grown plants. Ethidium bromide staining of rRNA was used as a loading control.

Enhanced Disease Resistance Conferred by *cpr22* Is Dependent on *EDS1*, *PAD4*, and *NDR1*

Whether *cpr22*-induced disease resistance requires *EDS1*, *PAD4*, or *NDR1* was then assessed by monitoring symptom development after inoculation with an oomycete or bacterial pathogen. Wild-type Ws and Col-0 plants were susceptible to *H. parasitica* biotype Emco5, with ~95% developing sporangiophores by 7 d after inoculation, whereas *cpr22/CPR22* plants were completely resistant (Table 3). Mutations in *PAD4*, *EDS1*, or *NDR1* suppressed *cpr22*-mediated enhanced resistance. *cpr22* heterozygous *pad4-1* or *eds1-1* homozygous plants exhibited similar susceptibility as wild-type plants or the *pad4-1* or *eds1-1* single mutant plants, respectively. *cpr22* heterozygous *ndr1-1* homozygous plants, like *ndr1-1* single mutants, displayed somewhat heightened susceptibility to Emco5, as reported previously (Yoshioka et al., 2001). *cpr22*-mediated resistance to the virulent bacterial pathogen *P. syringae* pv *maculicola* ES4326 also was suppressed by mutations in *EDS1*, *PAD4*, or *NDR1*. Although the *cpr22* single mutant displayed ~100-fold less bacterial growth than wild-type Ws or Col-0 plants, this resistance was lost in all three double mutants (Figure 8A). Thus, *cpr22*-induced resistance to virulent oomycete and bacterial pathogens appears to be mediated by one or more signaling pathway(s) that use both the CC-NBS-LRR signal transducer NDR1 and the TIR-NBS-LRR transducers EDS1 and PAD4.

Mutations in *EDS1*, *PAD4*, and *NDR1* Do Not Suppress *cpr22*-Induced SA Accumulation

SA is a critical signal for *R* gene–mediated resistance, and mutations in *EDS1*, *PAD4*, and *NDR1* have been shown to suppress its accumulation in certain *Arabidopsis*–pathogen interactions (Zhou et al., 1998; Feys et al., 2001; Shapiro and Zhang, 2001). Because *cpr22*-mediated resistance to *H. parasitica* is SA-dependent (Yoshioka et al., 2001), we tested whether the loss of resistance in *cpr22 eds1-1*, *cpr22 pad4-1*, or *cpr22 ndr1-1* double mutants was attributable to reduced SA production. Similar to the *cpr22/CPR22* mutant, all three double mutants contained threefold to sevenfold higher levels of SA than wild-type plants or the *eds1-1*, *pad4-1*, or *ndr1-1* single mutants (Figure 8B). Thus,

Table 2. Morphological Phenotype and *PR-1* Gene Expression in Progeny of Crosses between *cpr22* and *ndr1-1*, *pad4-1*, or *eds1-1* Plants

Cross[a]	Generation	Total No. of Plants	Morphology/*PR-1* Expression			Hypothesis[e]	χ^{2f}	P
			N[b]	*PR-1*$^+$/*cpr22*[c]	*PR-1*$^-$/wt[d]			
cpr22/CPR22 × *cpr22/CPR22*	F1	20	5	9	6	1:2:1	0.30	0.95 > P > 0.8
cpr22/CPR22 × *ndr1-1/ndr1-1*	F1	7	0	3	4	0:1:1	–	
	F2	43	10	22	11	1:2:1	0.43	0.95 > P > 0.8
cpr22/CPR22 × *pad4-1/pad4-1*	F1	24	0	10	14	0:1:1	–	
	F2	76	15	41	20	1:2:1	1.32	0.8 > P > 0.5
cpr22/cpr22 × *eds1-1/eds1-1*	F1	5	0	5	0	0:1:0	–	
	F2	47	10	26	11	1:2:1	0.59	0.95 > P > 0.8

[a] The pollen donor is indicated first and the accepting plant second.
[b] Nonviable plants.
[c] All plants showed typical *cpr22* morphology and constitutive expression of the *PR-1* gene.
[d] All plants showed morphology similar to wild-type plants and did not exhibit constitutive *PR-1* expression.
[e] Hypothesis: *cpr22* is inherited as a semidominant mutation that is lethal in the homozygous condition. The *NDR1*, *PAD4*, and *EDS1* genes are not required for *cpr22*-induced morphology or *PR-1* gene expression.
[f] Two degrees of freedom.

cpr22-induced SA accumulation is largely independent of *EDS1*, *PAD4*, and *NDR1*.

DISCUSSION

Here, we report the cloning of *cpr22*, an ~3-kb deletion mutant that generates a chimeric gene, *ATCNGC11/12*, by linking the putative ATCNGC-encoding genes *ATCNGC11* and *ATCNGC12*. Complementation studies and analysis of KO lines revealed that expression of *ATCNGC11/12* is required for the phenotype conferred by *cpr22*. However, because expression of a *ATCNGC12* transgene suppressed the phenotype conferred by *cpr22* in a dosage-dependent manner, the ratio between ATCNGC11/12 and ATCNGC12 also appears to be critical for phenotype development. Structural and functional analyses indicated that ATCNGC11/12, ATCNGC11, and ATCNGC12 are all functional cation channels. Based on these combined results, several mechanisms through which ATCNGC11/12 induces the phenotype conferred by *cpr22* can be envisioned. The first possibility is that ATCNGC11/12 activates the phenotype conferred by *cpr22* by destroying the function of CNCG12-containing channels. However, because ATCNGC12 single KO plants are almost indistinguishable from wild-type plants, this possibility seems unlikely. Instead, we suggest that ATCNGC11/12 competes with ATCNGC12 to form tetramer channels. In this scenario, there are two possibilities: the channels containing ATCNGC11/12 either gain an altered function or function as a constitutively active form of the original channels. Consistent with the latter possibility, *ATCNGC12* single KO plants exhibit reduced levels of resistance against an avirulent isolate of *H. parasitica*, compared with wild-type plants. Because this finding suggests that wild-type ATCNGC12 is a positive regulator of *R* gene–mediated resistance, expression of a constitutively active form of ATCNGC12 (in the form of ATCNGC11/12) would likely confer enhanced pathogen resistance.

The demonstration that the resistance to *H. parasitica* Emwa1 was comparably suppressed in *ATCNGC11* and *ATCNGC12* single KO plants as well as in their F1 progeny suggests that ATCNGC11, like ATCNGC12, is a positive regulator of resistance and that these proteins may work cooperatively. Although others (Zhong et al., 2003) have suggested that plant ATCNGCs form heterotetramers and may cooperate based on results in nonplant systems, our results indicate that such cooperation exists in plants. Although ATCNGC11 and ATCNGC12 are similar and may cooperate, their functions do not appear to be identical. Expression of a *ATCNGC12* transgene driven by its endogenous promoter suppressed *cpr22*-related phenotypes, whereas expression of a *ATCNGC11* transgene did not. Unfortunately, because the expression levels of the *ATCNGC11* and *ATCNGC12* transgenes cannot be determined because of the presence of their endogenous copies, it remains unclear whether this result reflects a functional difference between these ATCNGCs or is attributable simply to different expression levels. Stronger evidence that *ATCNGC11* and *ATCNGC12* have at least some functional differences comes from the demonstration that *ATCNGC11/12*-induced lesion formation in *N. benthamiana* was suppressed by *ATCNGC12* but not by *ATCNGC11*.

Table 3. Resistance Status of *cpr22* Single and Double Mutants to *H. parasitica* Isolate Emco5

Genotype	Total No. of Plants	No. of Plants[a]		Plants (%)[b]
		R	S	
CPR22/CPR22 (Ws)	70	5	65	92.9
CPR22/CPR22 (Col-0)	32	2	30	93.7
cpr22/CPR22	76	76	0	0.0
CPR22/CPR22/pad4-1/pad4-1	63	8	55	87.3
cpr22/CPR22/pad4-1/pad4-1	93	8	85	82.7
CPR22/CPR22/eds1-1/eds1-1	42	0	42	100.0
cpr22/CPR22/eds1-1/eds1-1	35	5	30	85.7
CPR22/CPR22/ndr1-1/ndr1-1	20	0	20	100.0
cpr22/CPR22/ndr1-1/ndr1-1	28	0	28	100.0

[a] Based on formation of sporangiophores. R, resistance; S, susceptible.
[b] Percentage of plants that show formation of sporangiophores.

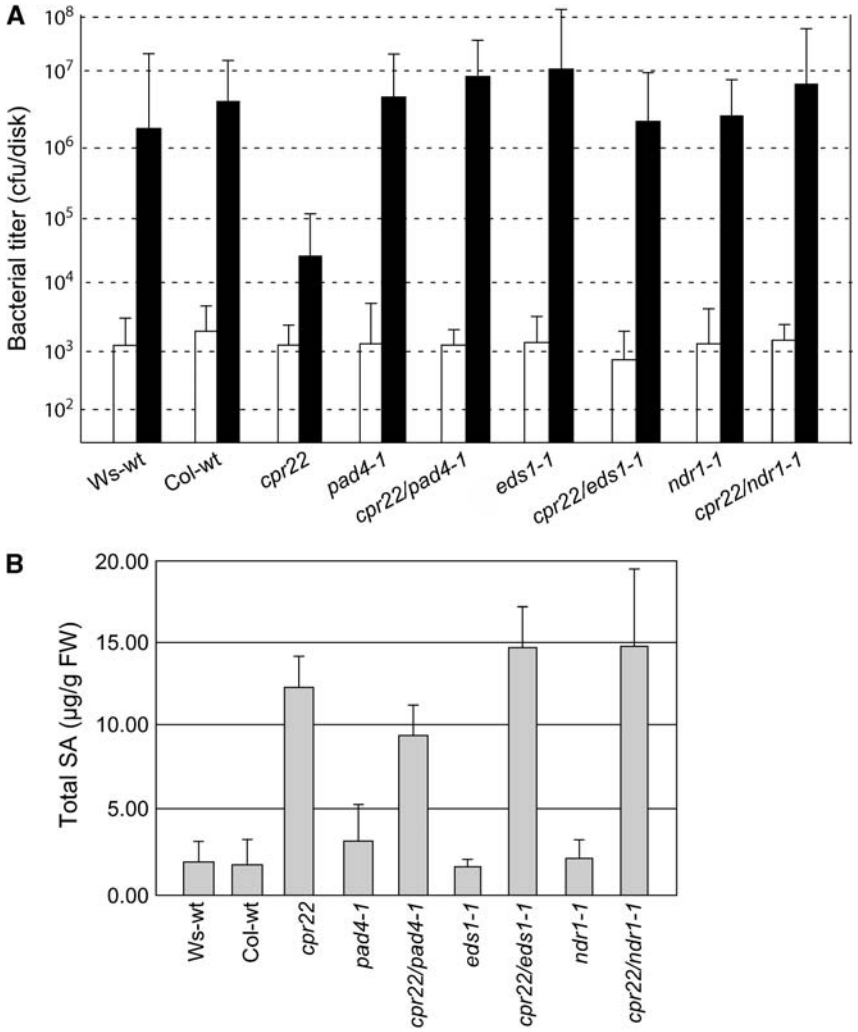

Figure 8. *EDS1*, *PAD4*, and *NDR1* Are Required for *cpr22*-Mediated Resistance to *P. syringae* pv *maculicola* ES4326 but Not for SA Accumulation.

(A) After infiltration with *P. syringae* pv *maculicola* ES4326, bacterial growth was monitored in the leaves of 3-week-old wild-type Ws and Col-0 plants, *cpr22/CPR22*, *eds1-1*, *pad4-1*, and *ndr1-1* single mutants, and *cpr22* heterozygous, *ndr1-1*, *pad4-1*, or *eds1-1* homozygous double mutant plants by collecting three leaf discs at 0 d after inoculation (open bars) and 3 d after inoculation (closed bars). Colony-forming units (cfu) are expressed ±SD and represent averages of four independent samples.

(B) Total SA levels were assayed in leaves of 3-week-old, soil-grown wild-type Ws and Col-0 plants, *cpr22/CPR22* (*cpr22*), *eds1-1*, *pad4-1*, and *ndr1-1* single mutants, and *cpr22* heterozygous, *ndr1-1*, *pad4-1*, or *eds1-1* homozygous double mutant plants. The values are presented in micrograms per gram fresh weight (FW) and represent averages ± SD of three samples consisting of leaves from three plants per line.

In addition to this study, there is growing evidence that ATCNGCs play a role in regulating defense response activation. In particular, mutations in *ATCNGC2* (*DND1*) and *ATCNGC4* (*HLM1*, *DND2*) confer constitutive *PR* gene expression, increased SA levels, and enhanced resistance to pathogens (Yu et al., 1998; Clough et al., 2000; Balague et al., 2003; Jurkowski et al., 2004). Despite these similarities with the phenotype conferred by *cpr22*, however, ATCNGC11/12, ATCNGC2, and ATCNGC4 do not appear to have identical roles in the resistance pathway. The *dnd1* mutant displays gene-for-gene disease resistance to avirulent pathogens in the absence of cell death (Yu et al., 2000), and the HR in *hlm1/dnd2* mutants is strongly reduced and/or delayed (Balague et al., 2003; Jurkowski et al., 2004). By contrast, HR cell death in *cpr22* was comparable to that displayed by wild-type plants after inoculation with *P. syringae* pv *tomato* carrying *avrRpt2*. In addition, our preliminary studies suggest that the expression patterns of *ATCNGC11/12*, *ATCNGC2*, and *ATCNGC4* and the patterns of spontaneous cell death exhibited by their respective mutants differ (K. Yoshioka and D.F. Klessig, unpublished data).

The ATCNGC gene family of *Arabidopsis* consists of 20 members whose overall genomic sequence similarity ranges from 55 to 83% (Maser et al., 2001). Based on sequence similarity, these genes have been divided into four groups, with

group IV the most distantly related to the other ATCNGCs. *ATCNGC2* and *ATCNGC4*, which are closely related to each other, are the sole members of subgroup IVB. By contrast, both *ATCNGC11* and *ATCNGC12* are only distantly related to these genes and are two of six genes belonging to group I. Interestingly, the calmodulin binding domain sequence in ATCNGC12 is significantly divergent from those of other ATCNGCs. This observation raises the possibility that *ATCNGC12* activity is regulated via a specific calmodulin that does not bind to other ATCNGCs.

In addition to *cpr22*, *dnd1*, and *hlm1*, several other *Arabidopsis* mutants that develop spontaneous lesions, constitutively express defense responses, and display enhanced disease resistance have been identified (Dempsey et al., 1999; Silva et al., 1999; Clough et al., 2000; Jambunathan et al., 2001; Yoshioka et al., 2001; Balague et al., 2003). Whether these resistance responses are activated via a signaling pathway(s) also used by some *R* genes or simply by perturbing critical cellular processes is unclear at present. However, several lines of evidence suggest that *cpr22* exerts at least some of its effects by stimulating pathways used by certain *R* genes. For example, the *ssi4* mutant, which contains a defect in a TIR-NBS-LRR–type gene, and transgenic plants overexpressing the resistance genes *RPW8.1* and *RPW8.2* also display humidity-sensitive, constitutive activation of defense responses and disease resistance (Shirano et al., 2002; Xiao et al., 2003; Zhou et al., 2004). Additionally, the demonstration that KO mutants lacking *ATCNGC11* or *ATCNGC12* display suppressed *R* gene–mediated resistance strongly suggests that *cpr22*-mediated resistance is activated by defense signaling pathways rather than by metabolic perturbation. Further supporting this hypothesis, genetic analysis revealed that the resistance signal transducers *EDS1*, *PAD4*, and *NDR1* are all required for *cpr22*-mediated enhanced disease resistance, although they are not required for *cpr22*-induced *PR* gene expression, SA accumulation, or spontaneous lesion formation. It is interesting that *dnd1*- and *dnd2*-induced resistance to virulent bacteria requires *PAD4*, whereas *PR* gene expression, SA accumulation, and disease resistance do not (Jirage et al., 2001). Because *PAD4* interacts with *EDS1* (Feys et al., 2001), it is likely that *dnd1*- and *dnd2*-induced resistance, like that of *cpr22*, requires *EDS1*; whether *NDR1* also is involved will require further epistatic analysis.

The finding that *cpr22*-mediated resistance requires not only *NDR1* but also *EDS1* and *PAD4* was unexpected. *EDS1*/*PAD4* and *NDR1* are generally thought to function in mutually exclusive pathways regulated by TIR-NBS-LRR or CC-NBS-LRR *R* genes, respectively (Aarts et al., 1998; Feys et al., 2001).

Other exceptions to this rule are *RPP4* in the Col-0 ecotype (an ortholog of *RPP5* in the Landsberg *erecta* ecotype) (van der Biezen et al., 2002) and *RPP5*. In cotyledons, these *R* genes mediate partial resistance to *H. parasitica* via a pathway that is fully dependent on *EDS1* and partially dependent on *NDR1* (Aarts et al., 1998; McDowell et al., 2000; van der Biezen et al., 2002). The discovery that *cpr22* induces strong resistance to virulent bacterial and oomycete pathogens in an *EDS1*-, *PAD4*-, and *NDR1*-dependent manner supports the idea that these distinct signaling pathways undergo cross-regulation. Moreover, because *RPP4* confers resistance to *H. parasitica* Emwa1 in the Col-0 ecotype and this resistance is compromised in *ATCNGC11* and *ATCNGC12* KO lines, it is tempting to speculate that these two ATCNGCs play a role in *RPP4*/*5*-mediated resistance. Whether their role in defense signaling is specific for *RPP4*/*5*-mediated resistance or is also part of other *R* gene–triggered defense signaling cascades remains to be determined.

Compared with enhanced disease resistance, *cpr22*-induced *PR-1* expression and SA accumulation were not affected by mutations in *EDS1*, *PAD4*, or *NDR1*. Because these three signal transducers are believed to mediate signaling through SA (Zhou et al., 1998), this result was surprising. Together, these results suggest that one or more SA-independent branches, in addition to the SA-dependent branch(es), functions downstream of these three signal transducers and is required for disease resistance, but not for some defense responses, such as *PR-1* expression.

In summary, our results suggest that ATCNGC11/12 induces pathogen resistance through multiple defense signaling pathways, whereas ATCNGC11 and ATCNGC12 function as positive components in one or more of these pathways. Although the mechanism by which ATCNGC11/12 activates resistance is currently unclear, ion fluxes are important early events in the defense signaling process. Further characterization of *ATCNGC11/12*, *ATCNGC11*, and *ATCNGC12* should provide important insights into the role(s) that ATCNGCs plays in transducing different signals after pathogen infection.

METHODS

Plant Growth Conditions

Arabidopsis thaliana plants were grown on Pro-Mix soil (Premier Horticulture) in a growth chamber under ambient humidity as described by Silva et al. (1999). For the high RH condition, 95% RH was applied.

Map-Based Cloning of *cpr22*

The *CPR22* locus was mapped using the F2 progeny from crosses between *cpr22*/*CPR22* (Ws ecotype) and either wild-type Col-0 or wild-type Landsberg *erecta* plants. Novel CAPS (Konieczny and Ausubel, 1993) and simple sequence length polymorphism (Bell and Ecker, 1994) markers were generated based on information from the CEREON polymorphism collection. Of 1355 F2 plants examined using these markers, one recombination event was identified using marker C424561 and four recombination events were identified using C424985. No recombination events were identified using additional markers within this 60-kb region. Thus, *CPR22* is located within a region spanning the end of BAC clone F11C10 and the beginning of F13A10. Specific PCR primers to amplify the putative ORFs in this 60-kb region were designed using the F11C10 and F13A10 sequences. The PCR products, generated using genomic DNA from wild-type WS or *cpr22* homozygous plants as the template, were sequenced directly using an automatic sequencer (ABI Prism model 3100).

PCR Analysis

To determine whether *ATCNGC11* is translated from an alternative start codon, PCR analysis was performed using genomic DNA from wild-type Ws plants and primers corresponding to several upstream ATG codons. The primers used were ATG1F (5′-ATGGAAAATTGAAAAGTGTTAGAGGA-3′), ATG2F (5′-ATGAACAAGTTTAACATAGCTTC-3′), and ATG3F (5′-ATGAATCTTCAGAGGAAAT-3′) as forward primers and UD1R1 (5′-GGTCTTCCTCCAGTAAACCT-3′) as the reverse primer. RT-PCR

also was performed with these primers using cDNA generated by SuperScript reverse transcriptase (Invitrogen Life Technologies) according to the manufacturer's instructions. Both PCR and RT-PCR products were sequenced. To isolate a cDNA of *ATCNGC11/12*, RT-PCR was performed using total RNA from *cpr22* homozygous plants and the primers Bam-ATG3F (5′-GGGATCCCATGAATCTTCAGAGGAGAAA-3′) and ORF14-R1-24 (5′-CTATGCTTCAGCCTTTGCAAACTC-3′). This cDNA was cloned into plasmid pGEM-T Easy (Promega) and sequenced by the same method described above.

Homozygous plants of KO lines were created by self-pollination and confirmed by PCR according to suggestions from the Salk Institute (http://signal.salk.edu/tdnaprimers.html) using primers LBb1 (5′-GCCTTTTCAGAAATGGATAAATAGCCTTGCTTCC-3′), 22RP (5′-CAGGCAAGAGAATGAAACCTTCAA-3′), 57RP (5′-TCACCCGGTAGGACATCCATTT-3′), 568RP2 (5′-TCAGTATCGTCGCCTCCATAG-3′), 22LP (5′-ATTGCTTTTGGTGGGGTCTCC-3′), 57LP (5′-CGTCGCTGGTGTCAGAGAGAA-3′), and 568LP (5′-GGTTGAGGTGGTGAGTATTCG-3′).

Expression of *ATCNGC11*, *ATCNGC12*, *ATCNGC11/12*, *PR-1*, and β-tubulin was monitored by RT-PCR using the following gene-specific primers: for *ATCNGC11*, cDNA-13-F1 (5′-AGGTTTACTGGAGGAAGACC-3′) and cDNA-13-R1 (5′-CTAGCGATCACATTACATAGAG-3′); for *ATCNGC12*, cDNA-14-F1 (5′-CGGGAAGATGAAAACACTGG-3′) and cDNA-14-R1 (5′-CACTATGCTTCAGCCTTTGC-3′); for *ATCNGC11/12*, cDNA-13-F1 and cDNA-14-R1; for *PR-1*, PR1-F (5′-AGCCTATCGTCACACTCCCGCTCAA-3′) and PR1-R (5′-GCTACAAATCACCCAAATATACTCA-3′); and for β-tubulin, β-tubulin-5′ (5′-CGTGGATCACAGCAATACAGAGCC-3′) and β-tubulin-3′ (5′-CCTCCTGCACTTCCACTTCGTCTTC-3′). cDNAs were generated by the same method described above.

Plant Transformation

A genomic *ATCNGC12* clone, containing 0.8 kb of 5′ promoter sequence and 0.5 kb of the 3′ untranslated region, and a genomic *ATCNGC11* clone, containing 1.0 kb of 5′ promoter sequence and 0.5 kb of untranslated region, were generated by PCR using primers NEWCLONE-F1BAM (5′-CTAGGATCCTAGCGAGAATCTCACCACCACAACCAC-3′) and NEWCLONE-R1ECO (5′-GCGAATTCGGTCTCTGAGCAGCAAAGGATCATAGCG-3′) for ATCNGC12 and primers CLONE13G-F1 (5′-GTTTCTTCAATTCTGTTGAC-3′) and D1R1 (5′-CCAGTGTTTTCATCTTCCCG-3′) for ATCNGC11. PCR was performed using *Pfu* DNA polymerase (Stratagene). The PCR product was cloned into pGEM-T Easy (Promega) and sequenced. This genomic *ATCNGC12* clone was then subcloned into pBIN19 (Clontech) and transformed into both *cpr22* homozygous and heterozygous plants using the vacuum infiltration method (Bechtold and Pelletier, 1998). Transformants were selected on Murashige and Skoog (1962) medium containing 50 μg/mL kanamycin and then transferred to soil. The presence of the introduced *ATCNGC12* or *ATCNGC11* clone and T-DNA region in the T1 and T2 progeny of *cpr22* homozygous transgenic plants was confirmed by PCR analysis. For the T1 and T2 progeny of *cpr22* heterozygous transformants, the presence of the introduced *ATCNGC12* or *ATCNGC11* clone and the endogenous *ATCNGC11/12* chimeric gene was determined by performing PCR analysis for full-length *ATCNGC12* or *ATCNGC11*, the T-DNA, full-length *ATCNGC11/12*, and the genomic region between *ATCNGC11* and *ATCNGC12*. To detect the T-DNA, the following specific primers were used: LBc-F (5′-ACGGGCAACAGCYGATT-3′) and LBc-R (5′-AGTTGCGCAGCCTGAAT-3′).

For stable transformation and transient expression, the cDNAs *ATCNGC11*, *ATCNGC12*, and *ATCNGC11/12* were subcloned into pMBP3 (Cambia). Stable transformation was performed as described above. *Agrobacterium tumefaciens*–mediated transient expression in *Nicotiana benthamiana* was performed as described by Sessa et al. (2000). *A. tumefaciens* strain GV2260 (final density of 0.2 OD_{600}) was used to syringe-infiltrate *N. benthamiana* leaves, and cell death was monitored at 3 d after infiltration.

Trypan Blue Staining

Leaf samples were taken from 2- to 3-week-old plants grown on soil. Trypan blue staining was performed as described previously (Bowling et al., 1994).

RNA Extraction and Gel Analysis

Small-scale RNA extraction was performed using the Trizol reagent (Gibco BRL) according to the manufacturer's instructions. RNA gel blot analysis and synthesis of random primed probes were performed as described previously (Shah et al., 1999). RNA gel blot hybridization was performed as described previously (Kachroo et al., 1995).

Functional Characterization of ATCNGCs in Yeast

ATCNGC11 cDNA in the pGEM plasmid (see above) was amplified by PCR using primers BamAtc11 (5′-CGGGATCCCGATGAATCTTCAGAGGAG-3′) and EcoAtc11 (5′-GGAATTCCCTAGGTTTCATCCATAGG-3′) and then subcloned into the pYES (Invitrogen) plasmid *Bam*HI and *Eco*RI sites. *ATCNGC12* and *ATCNGC11/12* cDNAs in the pGEM plasmid (see above) were restriction-digested with *Bam*HI and *Not*I and subcloned into the pYES plasmid. The K^+ uptake–deficient yeast (*trk1,2*) strain WD3 (Mat a; leu2-3, 2-112; trp1-1; ura3-3; ade2-1; his3-11; can1-100; trk1-LEU2; trk2-HIS3) was transformed with the empty plasmids pYES, pYES-ATCNGC11, pYES-ATCNGC12, and pYES-ATCNGC11/12 using the Qbiogene/Bio 101 EZ-Yeast transformation kit according to the manufacturer's protocol. Positive transformant colonies were selected on solid YNB-uracil (ura) medium (Qbiogene) supplemented with complete synthetic medium without ura (Qbiogene), $(NH_4)_2SO_4$ as a nitrogen source, glucose as a carbon source, and 100 mM KCl. Transformed yeast strains were maintained (−80°C) as 25% (w/v) glycerol stocks, and freshly streaked cultures were generated from the glycerol stocks on solid YNB-ura. For each experiment, liquid YNB-ura cultures were inoculated from solid YNB-ura medium plates. Colonies on solid plates were never >4 weeks old, to prevent suppressor and revertant mutations. The *trk1,2* complementation assay followed the method described by Mercier et al. (2004). YNB-ura liquid cultures of transformants were grown with shaking at 30°C for 24 h. Aliquots were pelleted by microcentrifuge and rinsed with sterile water. The concentrations of aliquots (100 μl) of the yeast cultures were adjusted, and the aliquots were then applied to assay plates containing YPGal (1% yeast extract, 2% peptone, and 2% galactose as a carbon source) with 0.07 mg/mL hygromycin B using glass beads to facilitate equal distribution across the surface. Sterile 3 M KCl (300 μl) was added to 1-cm-diameter filter disks (740-E; Schleicher & Schuell) under sterile conditions, and the filter disks were added to the assay plates. Assay plates were incubated in the dark at room temperature for 3 to 4 d. Complementation of K^+ uptake–deficient WD3 yeast strain growth was evaluated as colony formation around the 3 M KCl filter disks on each assay plate. When added to the YPGal assay medium, cAMP and/or cGMP were provided as dibutyryl (lipophilic) analogs at 100 μM final concentration.

Double Mutant Isolation

Double mutant lines were generated using the pollen from a *cpr22/CPR22* plant to fertilize a *pad4-1* homozygous (Col-0 ecotype) plant and the pollen from a *cpr22/cpr22* plant grown in high RH to fertilize an *eds1-1* (Ws ecotype) homozygous plant. Construction of *cpr22/CPR22; ndr1-1/ndr1-1* plants was as described by Yoshioka et al. (2001). Simple

sequence length polymorphism and CAPS marker analyses were done in the F1 generation to score for a successful cross between the *cpr22* mutant and *pad4-1* or *eds1-1*. The genotypes of F1, F2, and F3 progeny at the *PAD4* locus were determined by *Bsm*F1 digestion of a 1620-bp PCR fragment using the CAPS primers Pad4F (5′-ATGGACGATTGTCGATTCG-3′) and Pad4R (5′-CTCCATTGCGTCACTCTCAT-3′). The genotype at the *EDS1* locus was determined by digesting a 710-bp fragment amplified using the primers EDS3f (5′-GGATAGAAGATGAATACAAGCC-3′) and EDS1r (5′-ACCTAAGGTTCAGGTATCTGT-3′) with *Mse*I.

Pathogen Infection

Infection with *Hyaloperonospora parasitica* isolates Emco5, Emwa1, or Noco2 was performed by applying a single drop of asexual inoculum suspension (10^6 conidiosporangia/mL) per cotyledon of 7-d-old seedlings. The seedlings were grown at 16°C and >90% RH with an 8-h photoperiod. Plants whose leaves displayed sporangiophores were scored as susceptible at 7 d after inoculation. Infection with *Pseudomonas syringae* pv *maculicola* ES4326 was performed on 4-week-old soil-grown plants as described previously (Shah et al., 1997). Leaves were infiltrated with a bacterial suspension ($OD_{600} = 0.002$) in 10 mM $MgCl_2$, and colony-forming units were counted at 3 d after inoculation.

Extraction and Analysis of SA

Total SA was extracted from ~0.5 g of leaf tissue, and levels were determined as described by Bowling et al. (1994).

Accession Numbers

Sequence data for ATCNGC11 and ATCNGC12 can be found in the GenBank/EMBL data libraries under the following accession numbers: H84902 (At2g46440) and A84902 (At2g46450), respectively.

Supplemental Data

The following materials are available in the online version of this article.

Supplemental Figure 1. Analysis of T-DNA Insertion Lines and Their F1 Progeny.

Supplemental Figure 2. Morphology of Wild-Type Ws Plants Transformed with *ATCNGC11* and *ATCNGC12* Driven by the CaMV 35S Promoter.

ACKNOWLEDGMENTS

We thank J.E. Parker for *eds1-1* seeds, P. Repetti and B.J. Staskawicz for *ndr1-1* seeds and marker information, CEREON for information on the polymorphism, and the Salk Institute for T-DNA insertion lines. We gratefully acknowledge D'Maris Dempsey for critical reading of the manuscript and fruitful discussions. We also acknowledge Yumiko Shirano, Hui-ju Wu, and Fasong Zhou for helpful advice. This work was supported by Grant MCB-0110404 from the National Science Foundation to D.F.K. and by a Discovery Grant from the Science and Engineering Research Council of Canada to K.Y.

Received October 15, 2005; revised November 24, 2005; accepted December 27, 2005; published February 3, 2006.

REFERENCES

Aarts, N., Metz, M., Holub, E., Staskawicz, B.J., Daniels, M.J., and Parker, J.E. (1998). Different requirements for EDS1 and NDR1 by disease resistance genes define at least two *R* gene-mediated signaling pathways in *Arabidopsis.* Proc. Natl. Acad. Sci. USA **95,** 10306–10311.

Arazi, T., Sunkar, R., Kaplan, B., and Fromm, H. (1999). A tobacco plasma membrane calmodulin-binding transporter confers Ni^{2+} tolerance and Pb^{2+} hypersensitivity in transgenic plants. Plant J. **20,** 171–182.

Atkinson, M.M., Keppler, L.D., Orlandi, E.W., Baker, C.J., and Mischke, C.F. (1990). Involvement of plasma membrane calcium influx in bacterial induction of the K^+/H^+ and hypersensitive responses in tobacco. Plant Physiol. **92,** 215–221.

Atkinson, M.M., Midland, S.L., Sims, J.J., and Keen, N.T. (1996). Syringolide 1 triggers Ca^{2+} influx, K^+ efflux, and extracellular alkalization in soybean cells carrying the disease-resistance gene *Rpg4.* Plant Physiol. **112,** 297–302.

Balague, C., Lin, B., Alcon, C., Flottes, G., Malmstrom, S., Kohler, C., Neuhaus, G., Pelletier, G., Gaymard, F., and Roby, D. (2003). HLM1, an essential signaling component in the hypersensitive response, is a member of the cyclic nucleotide-gated channel ion channel family. Plant Cell **15,** 365–379.

Bechtold, N., and Pelletier, G. (1998). *In planta Agrobacterium*-mediated transformation of adult *Arabidopsis thaliana* plants by vacuum infiltration. Methods Mol. Biol. **82,** 259–266.

Bell, C.J., and Ecker, J.R. (1994). Assignment of 30 microsatellite loci to the linkage map of Arabidopsis. Genomics **19,** 137–144.

Bihler, H., Slayman, C.L., and Bertl, A. (2002). Low-affinity potassium uptake by *Saccharomyces cerevisiae* is mediated by NSC1, a calcium-blocked non-specific cation channel. Biochim. Biophys. Acta **1558,** 109–118.

Bowling, S.A., Guo, A., Cao, H., Gordon, A.S., Klessig, D.F., and Dong, X. (1994). A mutation in Arabidopsis that leads to constitutive expression of systemic acquired resistance. Plant Cell **6,** 1845–1857.

Cao, H., Bowling, S.A., Gordon, A.S., and Dong, X. (1994). Characterization of an Arabidopsis mutant that is nonresponsive to inducers of systemic acquired resistance. Plant Cell **6,** 1583–1592.

Century, K.S., Holub, E.B., and Staskawicz, B.J. (1995). NDR1, a locus of *Arabidopsis thaliana* that is required for disease resistance to both a bacterial and a fungal pathogen. Proc. Natl. Acad. Sci. USA **92,** 6597–6601.

Chandra, S., Stennis, M., and Low, P.S. (1997). Measurement of Ca^{2+} fluxes during elicitation of the oxidative burst in aequorin-transformed tobacco cells. J. Biol. Chem. **272,** 28274–28280.

Clough, S.J., Fengler, K.A., Yu, I.C., Lippok, B., Smith, R.K., Jr., and Bent, A.F. (2000). The Arabidopsis dnd1 ''defense, no death'' gene encodes a mutated cyclic nucleotide-gated ion channel. Proc. Natl. Acad. Sci. USA **97,** 9323–9328.

Creutz, C.E., Tomsig, J.L., Snyder, S.L., Gautier, M.C., Skouri, F., Beisson, J., and Cohen, J.J. (1998). The copines, a novel class of C2domain-containing, calcium-dependent, phospholipid-binding proteins conserved from Paramecium to humans. J. Biol. Chem. **273,** 1393–1402.

Delaney, T.P., Friedrich, L., and Ryals, J.A. (1995). Arabidopsis signal transduction mutant defective in chemically and biologically induced disease resistance. Proc. Natl. Acad. Sci. USA **2,** 6602–6606.

Dempsey, D., Shah, J., and Klessig, D.F. (1999). Salicylic acid and disease resistance in plants. Crit. Rev. Plant Sci. **18,** 547–575.

Doke, N., Miura, Y., Sanchez, L.M., Park, H.J., Noritake, T., Yoshioka, H., and Kawakita, K. (1996). The oxidative burst protects plants against pathogen attack: Mechanism and role as an emergency signal for plant bio-defence. Gene **179,** 45–51.

Feys, B.J., Moisan, L.J., Newman, M.-A., and Parker, J.E. (2001). Direct interaction between the Arabidopsis disease resistance signaling proteins, EDS1 and PAD4. EMBO J. **20,** 5400–5411.

Flor, H. (1971). Current status of gene-for-gene concept. Annu. Rev. Phytopathol. **9,** 275–296.

Gaber, R.F., Styles, C.A., and Fink, G.R. (1988). *TRK1* encodes a plasma membrane protein required for high-affinity potassium transport in *Saccharomyces cerevisiae.* Mol. Cell. Biol. **8,** 2848–2859.

Glazebrook, J. (1999). Genes controlling expression of defense responses in Arabidopsis. Curr. Opin. Plant Biol. **2,** 280–286.

Glazebrook, J. (2001). Genes controlling expression of defense responses in Arabidopsis—2001 status. Curr. Opin. Plant Biol. **4,** 301–308.

Glazebrook, J., Rogers, E.E., and Ausubel, F.M. (1996). Isolation of Arabidopsis mutants with enhanced disease susceptibility by direct screening. Genetics **143,** 973–982.

Hammond-Kosack, K.E., and Jones, J.D.G. (1996). Resistance gene-dependent plant defense responses. Plant Cell **8,** 1773–1791.

Hua, J., Grisafi, P., Cheng, S.-H., and Flink, G.R. (2001). Plant growth homeostasis is controlled by the Arabidopsis BON1 and BAP1 genes. Genes Dev. **15,** 2263–2272.

Jabs, T., Tschöpe, M., Colling, C., Hahlbrock, K., and Scheel, D. (1997). Elicitor-stimulated ion fluxes and O_2^- from the oxidative burst are essential components in triggering defense gene activation and phytoalexin synthesis in parsley. Proc. Natl. Acad. Sci. USA **94,** 4800–4805.

Jambunathan, N., Siani, J.M., and McNellis, T.W. (2001). A humidity-sensitive Arabidopsis copine mutant exhibits precocious cell death and increased disease resistance. Plant Cell **13,** 2225–2240.

Jirage, D., Zhou, N., Cooper, B., Clarke, J.D., Dong, X., and Glazebrook, J. (2001). Constitutive salicylic acid-dependent signaling in *cpr1* and *cpr6* mutants requires *PAD4.* Plant J. **26,** 395–407.

Jurkowski, G.I., Smith, R.K., Jr., Yu, I.C., Ham, J.H., Sharma, S.B., Klessig, D.F., Fengler, K.A., and Bent, A.F. (2004). Arabidopsis DND2, a second cyclic nucleotide-gated ion channel gene for which mutation causes the ''defense, no death'' phenotype. Mol. Plant Microbe Interact. **17,** 511–520.

Kachroo, P., Leong, S.A., and Chattoo, B.B. (1995). Mg-SINE: A short interspersed nuclear element from the rice blast fungus, *Magnaporthe grisea.* Proc. Natl. Acad. Sci. USA **92,** 11125–11129.

Kaupp, U.B., and Seifert, R. (2002). Cyclic nucleotide-gated ion channels. Physiol. Rev. **82,** 769–824.

Keen, N.T. (1990). Gene-for-gene complementarity in plant-pathogen interactions. Annu. Rev. Genet. **24,** 447–463.

Ko, C.H., and Gaber, R.F. (1991). *TRK1* and *TRK2* encode structurally related K^+ transporters in *Saccharomyces cerevisiae.* Mol. Cell. Biol. **11,** 4266–4273.

Kohler, C., Merkle, T., and Neuhaus, G. (1999). Characterization of a novel gene family of putative cyclic nucleotide- and calmodulin-regulated ion channels in *Arabidopsis thaliana.* Plant J. **18,** 97–104.

Kohler, C., and Neuhaus, G. (2000). Characterization of calmodulin binding to cyclic nucleotide-gated ion channels from *Arabidopsis thaliana.* FEBS Lett. **14,** 133–136.

Konieczny, A., and Ausubel, F.M. (1993). A procedure for mapping Arabidopsis mutations using co-dominant ecotype-specific PCR-based markers. Plant J. **4,** 403–410.

Lemtiri-Chlieh, F., and Berkowitz, G.A. (2004). Cyclic adenosine monophosphate regulates calcium channels in the plasma membrane of Arabidopsis leaf guard and mesophyll cells. J. Biol. Chem. **279,** 35306–35312.

Leng, Q., Mercier, R.W., Yao, W., and Berkowitz, G.A. (1999). Cloning and first functional characterization of a plant cyclic nucleotide-gated cation channel. Plant Physiol. **121,** 753–761.

Levine, A., Pennell, R.I., Alvarez, M.E., Palmer, R., and Lamb, C. (1996). Calcium-mediated apoptosis in a plant hypersensitive disease resistance response. Curr. Biol. **6,** 427–437.

Madrid, R., Gomez, M.J., Ramos, J., and Rodriquez-Navarro, A. (1998). Ectopic potassium uptake in *trk1 trk2* mutants of *Saccharomyces cerevisiae* correlates with a highly hyperpolarized membrane potential. J. Biol. Chem. **273,** 14838–14844.

Maser, P., et al. (2001). Phylogenetic relationships within cation transporter families of Arabidopsis. Plant Physiol. **126,** 1646–1667.

McDowell, J.M., Cuzick, A., Can, C., Beynon, J., Dangl, J.L., and Holub, E.B. (2000). Downy mildew (*Peronospora parasitica*) resistance genes in Arabidopsis vary in functional requirements for NDR1, EDS1, NPR1 and salicylic acid accumulation. Plant J. **22,** 523–529.

Mercier, R.W., Rabinowitz, N.M., Ali, R., Gaxiola, R.A., and Berkowitz, G.A. (2004). Yeast hygromycin sensitivity as a functional assay of cyclic nucleotide gated cation channels. Plant Physiol. Biochem. **42,** 529–536.

Murashige, T., and Skoog, F. (1962). A revised medium for rapid growth and bioassays with tobacco tissue culture. Physiol. Plant. **15,** 473–497.

Nawrath, C., and Metraux, J.P. (1999). Salicylic acid induction-deficient mutants of Arabidopsis express *PR-2* and *PR-5* and accumulate high levels of camalexin after pathogen inoculation. Plant Cell **11,** 1393–1404.

Parker, J.E., Holub, E.B., Frost, L.N., Falk, A., Gunn, N.D., and Daniels, M.J. (1996). Characterization of *eds1*, a mutation in Arabidopsis suppressing resistance to *Peronospora parasitica* specified by several different *RPP* genes. Plant Cell **8,** 2033–2046.

Raz, V., and Fluhr, R. (1992). Calcium requirement for ethylene-dependent responses. Plant Cell **4,** 1123–1130.

Ryals, J.A., Neuenschwander, U.H., Willits, M.G., Molina, A., Steiner, H.-Y., and Hunt, M.D. (1996). Systemic acquired resistance. Plant Cell **8,** 1809–1819.

Sasabe, M., Takeuchi, K., Kamoun, S., Ichinose, Y., Govers, F., Toyoda, K., Shiraishi, T., and Yamada, T. (2000). Independent pathways leading to apoptotic cell death, oxidative burst and defense gene expression in response to elicitin in tobacco cell suspension culture. Eur. J. Biochem. **267,** 5005–5013.

Sessa, G., D'Ascenzo, M., and Martin, G.B. (2000). Thr38 and Ser198 are Pto autophosphorylation sites required for the AvrPto-Pto-mediated hypersensitive response. EMBO J. **19,** 2257–2269.

Shah, J., Kachroo, P., and Klessig, D.F. (1999). The Arabidopsis *ssi1* mutation restores pathogenesis-related gene expression in *npr1* plants and renders defensin gene expression salicylic acid dependent. Plant Cell **11,** 191–206.

Shah, J., Tsui, F., and Klessig, D.F. (1997). Characterization of a salicylic acid-insensitive mutant (*sai1*) of *Arabidopsis thaliana*, identified in a selective screen utilizing the SA-inducible expression of the *tms2* gene. Mol. Plant Microbe Interact. **10,** 69–78.

Shapiro, A.D., and Zhang, C. (2001). The role of *NDR1* in avirulence gene-directed signaling and control of programmed cell death in Arabidopsis. Plant Physiol. **127,** 1089–1101.

Shirano, Y., Kachroo, P., Shah, J., and Klessig, D.F. (2002). A gain-of-function mutation in an Arabidopsis Toll Interleukin1 receptor-nucleotide binding site-leucine-rich repeat type R gene triggers defense responses and results in enhanced disease resistance. Plant Cell **14,** 3149–3162.

Silva, H., Yoshioka, K., Dooner, H.K., and Klessig, D.F. (1999). Characterization of a new Arabidopsis mutant exhibiting enhanced disease resistance. Mol. Plant Microbe Interact. **12,** 1053–1063.

Talke, I.N., Blaudez, D., Maathuis, F.J.M., and Sanders, D. (2003). ATCNGCs: Prime targets of plant cyclic nucleotide signaling? Trends Plant Sci. **8,** 286–293.

van der Biezen, E.A., Freddie, C.T., Kahn, K., Parker, J.E., and Jones, J.D. (2002). Arabidopsis *RPP4* is a member of the *RPP5* multigene family of TIR-NB-LRR genes and confers downy mildew resistance through multiple signalling components. Plant J. **29,** 439–451.

Xiao, S., Brown, S., Patrick, E., Brearley, C., and Turner, J.G. (2003). Enhanced transcription of the Arabidopsis disease resistance genes *RPW8.1* and *RPW8.2* via a salicylic acid-dependent amplification circuit is required for hypersensitive cell death. Plant Cell **15,** 33–45.

Xu, H., and Heath, M.C. (1998). Role of calcium in signal transduction during the hypersensitive response caused by basidiospore-derived infection of the cowpea rust fungus. Plant Cell **10,** 585–598.

Yoshioka, K., Kachroo, P., Tsui, F., Sharma, S.B., Shah, J., and Klessig, D.F. (2001). Environmentally-sensitive, SA-dependent defense response in the *cpr22* mutant of Arabidopsis. Plant J. **26,** 447–459.

Yu, I.C., Fengler, K.A., Clough, S.J., and Bent, A.F. (2000). Identification of Arabidopsis mutants exhibiting an altered hypersensitive response in gene-for-gene disease resistance. Mol. Plant Microbe Interact. **13,** 227–286.

Yu, I.C., Parker, J., and Bent, A.F. (1998). Gene-for-gene disease resistance without the hypersensitive response in Arabidopsis *dnd1* mutant. Proc. Natl. Acad. Sci. USA **95,** 7819–7824.

Zagotta, W.N., and Siegelbaum, S.A. (1996). Structure and function of cyclic nucleotide-gated channels. Annu. Rev. Neurosci. **19,** 235–263.

Zhong, H., Lai, J., and Yau, K.W. (2003). Selective heteromeric assembly of cyclic nucleotide-gated channels. Proc. Natl. Acad. Sci. USA **100,** 5509–5513.

Zhou, F., Menke, F.L., Yoshioka, K., Moeder, W., Shirano, Y., and Klessig, D.F. (2004). High humidity suppresses ssi4-mediated cell death and disease resistance upstream of MAP kinase activation, H_2O_2 production and defense gene expression. Plant J. **39,** 920–932.

Zhou, N., Tootle, T.L., Tsui, F., Klessig, D.F., and Glazebrook, J. (1998). PAD4 functions upstream from salicylic acid to control defense responses in Arabidopsis. Plant Cell **10,** 1021–1030.

Zufall, F., Firestein, S., and Shepherd, G.M. (1994). Cyclic nucleotide-gated ion channels and sensory transduction in olfactory receptor neurons. Annu. Rev. Biophys. Biomol. Struct. **23,** 577–607.